

Variability and complexity in calcite-based plaster production: A case study from a Pre-Pottery Neolithic B infant burial at Tel Ro'im West and its implications to mortuary practices in the Southern Levant

David E. Friesem^{1,2*}, Marie Anton^{3,4}, Paula Waiman-Barak⁵, Ruth Shahack-Gross⁵, Dani Nadel¹

¹Zinman Institute of Archaeology, University of Haifa, Israel

²McDonald Institute for Archaeological Research, University of Cambridge, United-Kingdom

³École Doctorale d'Archéologie, Université Paris 1, Panthéon-Sorbonne, Paris, France.

⁴Musée de l'Homme, Éco-Anthropologie et Ethnologie, CNRS, UMR 7206, Paris, France

⁵Department of Maritime Civilizations, Leon Recanati Institute of Maritime Studies, University of Haifa, Israel

*Corresponding author

David E. Friesem – df360@cam.ac.uk

Abstract

The production of lime plaster is considered as one of the hallmarks of the Pre-Pottery Neolithic B [PPNB] period in the Southern Levant, where lime plaster has been used not only in architectural but also in mortuary contexts. In this study we investigate the technology used to produce plaster associated with an infant burial found in the PPNB layers at the site of Tel Ro'im West [TRW]. Bulk sediment samples and undisturbed impregnated sediment block samples were studied using Fourier Transform Infrared (FTIR) spectroscopy, micromorphology and micro-FTIR. In addition, we report the results of experimental heating of chalk and marl used as geological reference materials. The results indicate that plaster associated with the burial appears in various compositions, and that none of them is based on pyrogenic production of lime. Rather, these plaster materials are composed of calcite-based crushed/ground local marl and/or chalk that were mixed with anthropogenic remains including fired-clay aggregates, burnt (carbonised) chalk fragments, bones and vegetal matter (the latter clearly used as temper). The case study from TRW provides new insights regarding the production of non-pyrogenic calcite-based plasters in mortuary contexts during the PPNB. This study calls for a re-consideration of archaeological plaster technology: while in the field it is often assumed that PPNB plaster is a product of pyrotechnology our results suggest that in certain cases archaeologists should consider other, non-pyrogenic, technologies of plaster production. We argue for a more widespread use of non-pyrogenic calcite-based plaster than previously suggested, not only in architectural but

also in mortuary contexts. We discuss the social, ecological and technological roles plaster production played in PPNB societies in the Southern Levant.

Highlights:

- Calcite-based plaster is best studied through micromorphology and FTIR spectroscopy
- Experimental heating of chalk and marl did not result in production of lime
- Non-pyrogenic plaster made of crushed chalk/marl was used in a PPNB mortuary context
- Non-pyrogenic plaster has been more widespread than previously suggested
- Non-pyrogenic plaster visually resembles lime plaster but can be produced in less effort

Introduction

The production of lime plaster by prehistoric cultures evinces an important technological development associated with cultural innovation and the emergence of more complex forms of social organisation (Friesem et al., 2019). Archaeological evidence dated to the Levantine Middle Epipalaeolithic, ca. 18-15 thousand calibrated years before present [hereafter k cal. BP], suggests that lime plaster has been sporadically produced (Bar-Yosef and Goring-Morris, 1977; Kingery et al., 1988) with increasing and more diverse use during the Natufian (ca. 15-11.6 k cal. BP) (Perrot, 1966; Kingery et al., 1988; Perrot and Ladiray, 1988; Goring-Morris et al., 1997; Valla et al., 2007; Friesem et al., 2019). However, it was only during the Pre-Pottery Neolithic B [PPNB], beginning ca. 10.5 k cal. BP, that pyrotechnology for the production of lime plaster became fully established with widespread evidence for lime plaster in domestic use in architectural contexts as well as for ritual purposes, especially in mortuary contexts (Gourdin and Kingery, 1975; Kingery et al., 1988; Rollefson, 1990; Goren and Goldberg, 1991; Rollefson et al., 1992; Goren et al., 2001; Goring-Morris, 2002; Goring-Morris and Horwitz, 2007; Clarke, 2012; Poduska et al., 2012). It was even suggested that the production of lime plaster should be considered as one of the hallmarks of PPNB cultures in the Southern Levant (Gourdin and Kingery, 1975; Garfinkel, 1987; Kingery et al., 1988; Goren and Goldberg, 1991; Rollefson and Köhler-Rollefson, 1992; Goren et al., 2001; Goring-Morris, 2002; Clarke, 2012).

Certain technological knowledge and skills are essential in order to transform carbonate rocks (e.g., limestone) into lime plaster. The rocks are heated, usually in kilns, in order to maintain high temperatures for prolonged time. When exposed to high temperature (often $>800^{\circ}\text{C}$) calcium carbonate (CaCO_3) transforms into calcium oxide (CaO - also termed quicklime). While in historic periods the use of kilns for production of lime plaster is well evident (Boynton, 1980), kilns were rarely found in prehistoric sites (Goren and Goring-Morris, 2008; Toffolo et al., 2017). Experiments have demonstrated the ability to produce quicklime from pulverized rocks using an open fire reaching just about 800°C for an hour (Karkanias, 2007). Once produced at high temperature, the quicklime is slaked with water forming a paste composed of calcium hydroxide ($\text{Ca}[\text{OH}]_2$ also known as the mineral portlandite). The plasticity of slaked lime paste allows it to be shaped and applied on various surfaces. During slaking a wide range of materials can be added to the slaked lime in order for the plaster to obtain different characteristics. For example, added soil or sediment can improve the carbonation process and cementation of lime plaster (Goren and Goldberg, 1991; Karkanias, 2007; Friesem et al., 2019). Alternatively, the heating in tandem of limestone and silicate materials is known to produce calcium-silicate minerals that upon hydration ('slaking') obtain a hydraulic character to the plaster – the ability to harden under water (Artioli and Angelini, 2010; Regev et al., 2010b). This innovation is primarily attributed to the Romans who commonly used volcanic ashes (the so-called 'pozzolanic

material') to prepare hydraulic materials for harbour construction, among other purposes (Artioli and Angelini, 2010). After application, the slaked lime paste is left to dry, transforming into a microcrystalline and highly disordered calcite, completing the lime cycle (Boynton, 1980; Kingery et al., 1988; Shoval, 2003; Chu et al., 2008; Regev et al., 2010a; Weiner, 2010). Thus, chemically, physically and also visually, lime plaster cannot be easily distinguished from unheated calcite; both are composed of calcium carbonate, often appear in various shades of white-grey, and are hard substances. Several methods have been developed to overcome this identification problem.

Early studies already pointed out the variability within archaeological calcite-based plasters (e.g., Gourdin and Kingery, 1975; Kingery et al., 1988; Goren and Goldberg, 1991). Research into the stable isotopic composition of carbon and oxygen in plasters and cements showed distinctly different values between lime and limestone, often used to identify forgeries (Ayalon et al., 2004; Goren et al., 2004). Other studies looked into the micromorphology (Karkanas, 2007) and infrared spectroscopic properties (Regev et al., 2010a; Poduska et al., 2012) of lime plaster and developed further criteria by which lime plaster can be distinguished from other, non-pyrogenic, calcite-based plasters. These developments allowed identifying non-pyrogenic calcite-based plaster in several Bronze and Iron Age sites in the southern Levant (Friesem and Shahack-Gross, 2013; Goshen et al., 2017; Shahack-Gross, 2018).

Below we report on the first identification of PPNB non-pyrogenic calcite-based plaster, complemented by laboratory experiments, that enhances our understanding of archaeological plasters and demonstrates the variability and complexity of plaster technology in the past.

Identification and archaeological significance of plaster in the PPNB

The widespread evidence of lime plaster production and use in the Near East during the PPNB was approached from the material point of view since the 1980s, with a focus on the southern Levant. Studies found that PPNB plaster displays impure lime-based paste and in many cases it has been found to be only partly burnt (i.e., not fully transformed into quicklime) and partly carbonated (i.e., the quicklime did not fully react during slaking to form homogenous disordered micritic calcite), concluding that PPNB plaster was prepared from quicklime (pyrogenic calcite) (Kingery et al., 1988; Goren and Goldberg, 1991; Goren et al., 2001; Karkanas, 2007; Poduska et al., 2012; Toffolo et al., 2017). It has been suggested that lime plaster was produced on a large-scale, resulting in deforestation and exhaustion of trees around sites (Garfinkel, 1987; Rollefson, 1990; Rollefson and Köhler-Rollefson, 1992). Later studies rejected these suggestions arguing for less effort required for the production of PPNB lime plaster and a lower environmental effect in terms of felling and burning of trees (Goren and Goldberg, 1991; Goren et al., 2001; Karkanas, 2007; Goren and Goring-Morris, 2008; Rollefson,

2014). In all studies, the basic assumption was that all plaster found in PPNB sites is pyrogenic, based on the transformation of limestone into quicklime.

Generally, the use of PPNB plaster can be divided into two distinct contexts: domestic architecture (e.g., mainly plastered floors) and ritual or mortuary features (e.g., covering burials and plastered skulls). Goring-Morris (2002) argued that lime plaster played a major ritual role in PPNB communities bearing symbolic significance, whether in domestic and architectural contexts and certainly in mortuary contexts. Although the use of the plaster, and most probably the social arena of its production, differed between the two contexts, the technology employed was quite similar. The PPNB plaster is characterised by the production of an impure material composed of a mixture of partly burnt lime, local sediments and in some cases the addition of vegetal matter, iron minerals, gypsum, ash, bones, fired clay and dung (Gourdin and Kingery, 1975; Kingery et al., 1988; Goren and Goldberg, 1991; Goren et al., 2001; Goring-Morris and Horwitz, 2007; Goren and Goring-Morris, 2008; Poduska et al., 2012; Toffolo et al., 2017). The use of plaster in mortuary contexts dates back to the Natufian (Valla et al., 2007; Grosman et al., 2016). A recent discovery of a burial ground dating to 12 k cal. BP in Nahal Ein Gev II (Grosman et al., 2016) revealed a thick layer of lime plaster covering several burials and made of well-carbonated lime mixed with local sediment and partly burnt limestone (Friesem et al., 2019).

The aim of this study is to investigate the technology behind the complex plaster features directly associated with an infant burial found in the PPNB layers of Tel Ro'im West [TRW] in order to reconstruct the process of mortuary plaster production and discuss such contexts in the wider realm of symbolic behaviour during the Levantine PPNB. To do so, we applied multiple mineralogical and micromorphological analyses alongside laboratory experiments in order to generate high-resolution data on the material properties of the plaster. Based on the data reported here, we propose a novel reconstruction of non-pyrogenic, calcite-based, plaster production and its ritual use in the infant burial at TRW. Finally, we place our data and interpretation within a broader frame of early plaster technology in the Southern Levant.

The site

Tel Ro'im West is a small Neolithic mound situated above the northwestern margin of the Hula Valley, ca. 150 m west of Tel Ro'im (figure 1). It is located at the foot of the Ramim Ridge, ca. 175 m asl. Estimated at ~one hectare in size, the site seems to have been part of the dense settlement network that existed during most of the Neolithic period in the Hula Valley, particularly on the western and northern margins, and included sites such as Beisamoun (Lechevallier, 1978; Rosenberg et al., 2006;

Bocquentin et al., 2014; Khalaily et al., 2015), Hagoshrim (Getzov, 2008) and Tel Te'o (Eisenberg et al., 2001).

TRW was first discovered by the late Amnon Asaf, and initial probes led to a long salvage excavation season in 2004. The excavations focused on two areas: Area A (125 m²) and Area B (50 m²). Area A was excavated to bedrock and reached a depth of ca. 4 m, with the longest Neolithic stratified sequence; Area B was excavated to an average depth of ca. 1 m. The PPNB – Pottery Neolithic sequence at the site provided rich lithic and faunal assemblages, pottery remains, as well as stone architecture and human graves (Nadel and Nadler-Uziel, 2011; Nativ et al., 2014; Eshed and Nadel, 2015; Agha et al., 2019). Five main strata were identified (I–V) in Area A while in Area B only the top three strata (I–III) were exposed and studied. A plaster complex associated with a burial from Stratum V is the focus of this paper, and thus strata I–IV are only briefly presented.

Stratum I (0.5–1.0 m thick) is the surface layer consisting of brown modern field soil containing large boulders and isolated Neolithic finds.

Stratum II (0.5–1.0 m thick) is composed of brown sediment similar to that of Stratum I. It consists of a dusty clay loam, probably ash, mixed with brown clay; an abundance of stone, gravel and ceramic sherds is recorded. Two segments of a long wall, more than 1 m wide, were found. Stratum II is the uppermost occupational horizon, assigned to the Pottery Neolithic period. The flint assemblage appears to be Yarmukian, while the pottery has northern non-Yarmukian affinities (Nadel and Nadler-Uziel, 2011; Nativ et al., 2014).

Stratum III (0.5–1.0 m thick) is composed of very hard, brown to reddish-brown sediment, rich with gravel. A well-built curved wall was exposed along the eastern section and no archaeological finds were found beyond this wall, in areas E and F, possibly suggesting that it marked the settlement's eastern limit. Several building phases were discerned. The finds included very poorly preserved potsherds, flint tools, among them numerous deeply denticulated sickle blades, basalt crushing and grinding tools and a few bone implements. Based on the analysis of the flint tools, the stratum was associated with the Pottery Neolithic period. The flint assemblage appears to be Yarmukian, while the pottery has northern non-Yarmukian affinities (Nadel and Nadler-Uziel, 2011; Nativ et al., 2014).

Stratum IV (0.5–0.8 m thick) is composed of light coloured, yellowish-grey sandy sediment. Remains of a few rectangular walls were found, one of which was preserved to a height of up to three courses, and was particularly massive and at least 13 m in length. Based on the absence of potsherds and analysis of the flint assemblage this stratum was associated with the PPNC (Nadel and Nadler-Uziel, 2011).

Stratum V (0.5–1.2 m thick) is characterized by brown-red sediment. A few construction phases were found, mainly encompassing several levels of plastered flooring. Three burials were also found, one of which (B.2116, with the associated plaster complex P.2000) is the focus of this study. The flint assemblage was rich and differed from the upper assemblages in the types of tools, the knapping technology and the quality. This stratum was associated with the late PPNB. Under Stratum V, ca. 4 m below the surface, sterile red soil was found throughout the area.

The infant burial

A burial of an infant (B.2116) was found in Square J8, at ca. 171.80 m above sea level, near the northeastern corner of Area A (figure 2) (Eshed and Nadel, 2015). Above it was a large plaster floor (F.2100) which encompassed a semi-triangular feature paved with large stones, about 1.5 x 1.5 m (L.2107). Under this floor were a polished axe and several arrowheads. The plaster complex addressed here (P.2000) was about 45 x 45 cm in top view and about 25 cm in thickness (figure 3). Macroscopically it appeared to have included a variety of plaster types and other deposits, and some vertical slabs and plaster pieces creating an inner "box" or "basin". The infant skeleton was found on the north rim of this feature, with most bones placed on stones – the head on small stones and the body on fist-sized stones (figure 4). The density of finds during the excavation of the skeleton was very low, less than one find per liter, and most are small flints <1cm.

The skeleton was lying on the left side and partly on the chest, with his head turned to the left. The left elbow was hyper flexed under the chest. The skull was found on the left clavicle and hand, with the mandible disconnected. It appears that the skull has tilted towards the individual's chest during the decomposition of the body. The left ribs and the thoracic vertebrae kept an anatomical coherence after the disappearance of the flesh. This preservation state is unlikely for an infant individual in this position. It is possible that a structure, such as a pit limit (not preserved), has prevented the skeleton from collapsing to the left. The few bones related to the pelvis and the right leg were disturbed during the discovery of the burial. It is possible that the rest of the lower limbs, never found during the excavation, were disturbed in the past.

Most of the individual is represented by the left part of the body, with some bones from the right part of the pelvis and leg. The bones are not fused and most of the secondary centre of ossification is not present. As no teeth were found and bone measurements indicate length exceeding 40 fetal weeks, it appears that the infant has been born alive but could not have been more than two months old when he died (Maresh, 1970; Fazekas and Kósa, 1978; Schaefer et al., 2009).

Materials and Methods

Sampling strategy

A large field block containing the infant skeleton and the plaster feature was removed intact from the site and taken to the laboratory at the Zinman Institute of Archaeology (University of Haifa) where it was excavated and studied. Bulk sediment samples (n=14) were collected from different areas of the block in order to sample the range of colours, hardness, texture and structure displayed by the deposits associated with the burial (figure 5a and 5b). In addition, undisturbed monolithic sediment samples (n=4) representing the diversity of sediments around the burial were collected (figure 5c and 5d).

Fourier Transform Infrared (FTIR) spectroscopy

Bulk samples (n=14) were analyzed using Fourier Transform Infrared (FTIR) spectroscopy in order to identify the major mineral components for each sample (table 1). The spectra were collected using a Thermo iS5 FTIR spectrometer using the KBr method. Spectra were collected between 4000 and 250 cm^{-1} , at 4 cm^{-1} resolution and interpreted using an internal library of infrared spectra of archaeological materials (the Kimmel Center for Archaeological Science Infrared Standards Library, Weizmann Institute of Science). Evaluation of clay alteration due to exposure to high temperatures (>500°C) was based on the presence (unheated) or absence (heated) of absorption bands at 3695, 3625 and 915 cm^{-1} (Berna et al., 2007). To evaluate the atomic order/disorder in calcite associated to its formation mechanisms (e.g., geological, biological or pyrogenic), the ν_2 and ν_4 absorption bands, corresponding to 874 cm^{-1} and 713 cm^{-1} respectively, were studied by following changes in their height through repetitive grinding of samples where calcite is a major component (n=11) (Regev et al., 2010a).

Soil and sediment micromorphology

Undisturbed monolithic sediment samples (n=4) were sampled by removing small (ca. 5 X 5 cm) blocks of sediment into plastic cups. These were dried in an oven at 50°C for 24h and then impregnated with a mixture of polyester resin and acetone (4:1) and MEKP-hardener. The hardened blocks were then sliced and glued to a glass slide measuring 80x30 mm and polished to standard 30 μm thin sections. The thin sections were first scanned in high resolution (4000 DPI), with a modified Nikon Coolscan LS-8000 ED Film Scanner, under plane-polarized light (PPL) and cross-polarized light (XPL). Microscopic analysis of thin sections was carried out under magnification (X25 - X200) using a Zeiss Axio Imager petrographic microscope. Micromorphological descriptions follow the terminology of Stoops (2003). Results of the micromorphological analysis are summarised in table 2.

Fourier-Transform Infrared Micro-spectrometry (micro-FTIR)

All thin sections (n=4) were analysed using an Agilent Cary 610 FTIR microscope in order to identify the extent of alteration of the clay minerals. Measurements were conducted using Transmission mode with 64 scans. All spectra were obtained at 4cm^{-1} resolution using Agilent Resolution Pro software and interpreted using an internal library of infrared spectra of archaeological materials (the Institute for Archaeological Sciences, University of Tübingen). In order to examine the exposure of clay minerals to high temperatures, the extent of clay alteration was determined based on the presence/absence of absorption bands at 3695 and 3625 cm^{-1} (Haaland et al., 2017; Villagran et al., 2017). In total 13 infrared spectra were collected (table 3).

Experimental samples and analysis

TRW is situated on the Paleocene age Taqiye Formation, a clay-rich marl. Less than 1 km north of the site, the Eocene age Adulam & Timrat Formations, predominantly composed of chalk, can be found (based on a geological map by Sneh and Weinberger, 2014 Metulla sheet 2-II). Both rock types, marl and chalk, are likely sources for plaster preparation as they contain calcite.

Experiments have been conducted at the Laboratory for Sedimentary Archaeology, University of Haifa. We conducted experimental heating of a chalky facies of the Ghareb and Taqiye [G&T] Formation (Senonian-Paleocene age), collected near Yoqneam (based on a geological map by Segev and Sass, 2009 Atlit sheet 3-III). The rock was crushed and ground using a mortar and pestle, wetted by tap water and the wet (chunky) paste poured into six round containers (4 cm diameter) and dried in an oven at 50°C overnight. Each container was then heated separately in an electric furnace to target temperatures of 400 , 500 , 600 , 700 , 800 and 900°C , with each heating lasting for 4 hours followed by furnace shutdown and samples slowly cooling in the chamber overnight. Infrared spectra were prepared from each sample a few days after cooling down to room temperature. The samples in each container were then impregnated by polyester resin and petrographic thin sections were prepared. The thin sections were described petrographically using micromorphological criteria (Stoops, 2003).

Additionally, rock fragments from the G&T and the Adulam formations (the latter collected near Bat Shlomo, based on a geological map by Segev and Sass, 2009 Atlit sheet 3-III) were heated at 700 , 800 and 900°C for 2 hours. After cooling down to room temperature, each heated rock fragment was placed in a Pyrex beaker and tap water was added with the aim of testing the potential of lime plaster production.

Results

Bulk sediment samples

Experimental results

FTIR analysis indicated that the unheated G&T Formation is composed of calcite, clay and opal (figure 6a) and that unheated Adulam Formation is composed of calcite and opal. Calcite disintegration and presence of portlandite ($\text{Ca}[\text{OH}]_2$) were recorded following heating to 700, 800 and 900°C, yet, portlandite seems to be a minor component while other minerals (probably calcium silicates) formed the bulk of these heated rocks (figure 6b). The lime (portlandite) containing samples did not react in the expected manner following the addition of water: they did not produce an exothermic reaction nor did they soften and become plastic (workable) pastes.

Archaeological results

Mineralogical analysis via FTIR of bulk sediment samples associated with the infant burial showed that clay and calcite are the major components in all samples (table 1). The colour of the samples correlates with the relative abundance of clay and calcite, with brown-orange colours resulting from higher clay than calcite and shades ranging between white, yellow and pink resulting from higher calcite than clay. In all the samples, the clay component did not show clear signs of alteration due to exposure to temperatures higher than 500°C. This is based on the presence of absorbance bands at 3695, 3625 and 915 cm^{-1} , that evince the presence of structural water (hydroxyls) in the clay lattice (Berna et al., 2007). Samples that include calcite as the main mineral component (figure 7) were analysed through sequential grinding to produce grinding curves as a proxy for the atomic order of calcite following the procedure of Regev et al. (2010a). The results, plotted in reference to grinding curves (Regev et al., 2010a), indicate that all samples can be associated with a geogenic origin and therefore were not exposed to very high temperatures (>800°C) (Regev et al., 2010a; Poduska et al., 2012; Goshen et al., 2017; Toffolo et al., 2017; Friesem et al., 2019). Moreover, calcium silicates as those that formed in the heating experiments were not identified in any of the archaeological samples, indicating that if heating took place, it must have been below the detection limit of our analytical instruments (i.e., at a temperature lower than 700°C) which is also below the temperature required to produce quicklime. Only one sample, TRW 13, presents mid-range values suggesting some extent of atomic disorder (figure 7) which may either result from the presence of wood ash or a mixture of burnt and unburnt calcite (Regev et al., 2010a). Overall, the FTIR analysis did not provide evidence for high temperatures as one would have expected in deposits associated with pyrogenic lime plaster (Chu et al., 2008; Regev et al., 2010a, 2010b; Poduska et al., 2012; Goshen et al., 2017; Toffolo et al., 2017; Friesem et al., 2019).

Thin section analysis

Experimental results

Micromorphological observations on the experimental samples were conducted only on G&T samples. Unheated G&T as well as G&T rock heated to 400°C share similar features: The groundmass (matrix) is composed of calcitic clay, grey in PPL and XPL, and contains foraminifera fossils. The fossil shells are transparent (colorless) in PPL and high order grey-white in XPL (figures 8a-d). G&T rock heated to 500, 600 and 700°C display a yellowish-grey matrix (in both PPL and XPL) and the fossil shells appear orange-red in both PPL and XPL (figure 8e-h). G&T rock heated to 800 and 900°C display an orange-grey groundmass in PPL and high order grey in XPL that is typical of portlandite/lime plaster. The fossil shells are yellowish-red, possessing a very high relief relative to the groundmass (figures 8i-l). Notably, the fossil shells do not disintegrate at high temperature and are clearly visible in thin section (though they do undergo chemical and structural changes; see also Daghmehchi et al., 2017).

The microstructure of the samples prepared by crushing, wetting, drying and followed by heating is pelletal/crumblly as these are composed of crushed rounded grains (figure 8e). These samples are grain-supported thus dominated by packing voids, yet vesicles are notable and reflect the evaporation of water after the wetting of the samples prior to heating (figure 8g). The microstructure of the highly-fired samples is homogenous and massive (figure 8k).

Archaeological results

Sample TRW-15

This sample is a blocky, hard, white-yellow material associated with bulk sample TRW-5 (figure 5c). The sample was chosen to represent what appeared to the naked eye as the most evident man-made plaster associated with the infant burial due to its sharp lower and upper contacts. Mesoscopically, it appears primarily composed of poorly sorted sub-angular and sub-rounded grey rock fragments (figure 9a-b). Under the microscope the sample displayed a dense calcite-rich grey matrix that appeared in some areas more yellowish (figure 9c-d) and darker grey in others (figure 9e-f). Foraminifera fossils are embedded in the matrix showing pale yellow shells (figure 9c), presenting some resemblance to the experimental unheated (figure 8a) and heated to 400°C G&T reference rock (figure 8c). The matrix includes grains of rubified clay (ceramic-like). These were analysed using micro-FTIR, and their spectra indicated alteration due to exposure to high temperature (>500°C) (table 3). In addition, the matrix presents large fragments of chalk, a pelletal structure (figures 9d-e), embedded bones (figure 9e) and thin elongated moldic voids indicating the use of vegetal matter as temper (figure 9f). The matrix has complex microstructure with chambers, vesicles and vughs. Channels and fissures are infilled with clay hypocoatings showing no heat-alteration under the micro-FTIR (table 3). We define this material to be impure, non-pyrogenic, vegetal tempered plaster. The rock raw material was crushed, as evident from the pelletal structure, possibly heated to low temperature (~400°C) and

mixed with materials such as vegetal matter, burnt soil aggregates and bone fragments (table 2). The clay infilling and hypocoatings are secondary, from post-depositional low energy flows through cracks.

Sample TRW-16

Sample TRW-16 was produced from a grey layer associated with bulk sample TRW-4. This grey layer seems to cover the entire block and is overlain by a brown to orange sediment at the top of the block (figures 5a and 5c). Mesoscopically and under the microscope this plaster material displayed similarity to TRW-15 (figure 9), however its matrix is less yellowish, exhibiting a dark grey colour (figures 10c-f). Unlike TRW-15, this plaster includes unheated (as determined by micro-FTIR; table 3) sediment clasts composed of a clay-rich groundmass, sub-angular quartz silt, and organic matter (figures 10c-d). These are features that resemble those of Terra Rosa soil. Some of the clay-rich clasts show leaching out of the clay fraction forming clay hypocoating in voids (figure 10c). The various types of fossils present in the micritic matrix show colorless shells (figure 10e) as in the experimental unheated and heated to 400°C reference G&T rock (figures 8a-d). The pelletal structure indicates that in some parts pulverized chalk was used (figure 10f). This sample is interpreted as plaster made of pulverized and probably unburnt chalk, similar to TRW-15 but with higher degree of mixing with the local sediment and no vegetal temper (table 2).

Sample TRW-17

Sample TRW-17 was produced from a white pinkish material at the top of the block associated with bulk sample TRW-3 (figures 5a-b). This whitish material seems to be deposited above a brownish sediment (figure 5d). Under the microscope the thin section revealed a sharp contact between two matrices (figures 11a-b). One is predominantly white, composed of unsorted sub-rounded rock fragments within a white matrix, and the other is predominantly reddish composed of unsorted sub-angular and sub-rounded rock and sediment fragments within a reddish matrix that includes numerous thin elongated voids (figure 11b). Under the microscope, the former presents a calcite-rich dense matrix with a yellowish-pale grey colour (similar to TRW-15) showing pelletal structure (figure 11c), some non-altered clay aggregates (table 3) and a complex microstructure with relatively minor extent of clay infilling and hypocoatings. The second, reddish matrix, presents high similarity to the first, but has extensive clay infilling, hypocoatings and iron staining of the groundmass (figure 11d). This matrix also includes heat-altered clay aggregates based on micro-FTIR analysis (table 3). The enrichment in clay in the second matrix is gradually decreasing further away from the contact between the two matrices (figure 11b), suggesting that the clay infilling and hypocoating probably happened post-depositionally. The difference in mesoscopic structure between the two layers suggests that they indicate two separate depositional events. The contact between them is an elongated channel infilled

with non-altered clay, based on micro-FTIR analysis (table 3), i.e., a post-depositional channel that occurs along a weakness zone that separates the two paleo-surfaces. Throughout the thin section there are thin elongated moldic voids indicating the incorporation of vegetal temper (figure 11f). The lower part, away from the contact, is more yellowish in colour and may represent some degree of burning, or a tint due to presence of clay; FTIR spectra indicate no exposure to high temperatures (figures 11e and 11g). We suggest that this sample represents two phases of application of impure and non-pyrogenic plaster material. The contact between the two phases has been infilled with clay that infiltrated into the lower phase resulting in staining and a more reddish colour.

Sample TRW-18

Sample TRW-18 incorporates a grey layer (associated with TRW-13) and a brown orange sediment (associated with TRW-14) (figures 5b and 5d). The sharp contact observed between these two deposits during sampling is less clear in the thin section where a diffuse contact appears (figures 12a-b). Mesoscopically, the samples differ in colour, texture and structure: The grey layer is composed of moderately sorted white and red sub-rounded to sub-angular rock and sediment fragments, while the brown layer is composed of reddish peds with a few sub-angular rock fragments. Under the microscope, the grey layer is composed of a calcite-rich matrix with high abundance of clay-rich clasts, some showing heat-alteration based on micro-FTIR analysis (table 3), burnt chalk fragments and bone fragments (figures 12c, 12e-f). This matrix, sampled in bulk as TRW-13, was the only one to show higher calcite atomic disorder (figure 7). We therefore interpret this material as an impure plaster composed of a mixture of local sediment, burnt and partly burnt chalk, but with no evidence for the production of pyrogenic lime (table 2). The brown layer is dominated by a clay-rich groundmass, non-heat-altered based on micro-FTIR (table 3), with sub-angular quartz silt and organic matter mixed with micritic calcite displaying complex microstructure that includes chambers, channels, vesicles and vughs, clay infilling and hypocoating of voids (figure 12d). This matrix can be associated with brown orange sediment representing the local unburnt sediment (table 2).

Discussion

PPNB Plaster technology at Tel Ro'im West

The infant burial in TRW was found in direct association with a feature encompassing a range of plaster materials (p.2000). The paved feature (L.2107) above the burial is one of its kind found at the site, and the unique burial under it, with the visible variety of colored sediments/plasters and the youngest baby at the site appear to form one complex (figures 2, 3, 4). The sequence of applying the variety of colored plasters was only partially reconstructed, but the inhumation of the baby on top of feature

p.2000 indicates pre-planned association between the burial, the variety of the p.2000 plasters, and likely also the later cover by a plaster floor and a stone pavement.

The geoarchaeological analysis of the different plaster materials and the comparison to experimental references indicate that the rock raw material was insufficiently burnt, if at all. The FTIR analysis showed that the plaster calcitic matrix does not display the atomic disorder expected when calcite is exposed to very high temperatures (>800°C) for a few hours (Regev et al., 2010a) which are essential for producing quicklime. The exceptional one sample (TRW 13) yielded mid-range values of atomic disorder (table 1, figure 7) that correspond with calcite atomic disorder found in wood ash. Alternatively, this sample could represent a mixed assemblage of burnt and unburnt limestone. The latter scenario is further supported by micromorphological observations. Under the microscope, the various plaster materials exhibit a dense micritic matrix with fossils that evince the use of chalk or marl as the raw material (figures 9c and 10d-f). In comparison to the experimentally heated chalk and marl references, the fossils do not display features associated with exposure to temperatures higher than 500°C (figures 8a-d). Some areas in the plaster that show pelletal structure (figures 9d-e, 10f, 11c and 11e) could be linked to the chalk/marl being pulverized (figures 8c-f). No microscopic evidence for unreacted lime (c.f., Karkanias, 2007; Goshen et al., 2017) was found within the plaster materials and the presence of partially-burnt chalk fragments (figures 10f and 12e) is therefore interpreted as an addition to a non-fired pulverized chalk (geogenic) putty. We cannot rule out the possibility that the raw material rock was burnt at very low temperatures, but a functional reason behind such a practice is unclear as quicklime is not produced at low temperatures. Even if the raw material was slightly burnt at low temperatures we do not consider it to be a pyrogenic material since it was not altered by heat.

The matrix of the different plaster materials all display a wide range of added materials, including: soil (figures 9c-d, 10c, 11d and 12c-f), bone fragments (figure 9e), rubified soil (ceramic-like) aggregates (figures 9b, 11b and 12b) and vegetal matter (figures 9f and 11e-f). Except for the vegetal matter that appears to be an intentional addition, it is unclear whether or not the other materials have been added purposefully or inadvertently. For instance, fired clay aggregates (ceramic-like) features were reported in association with plaster production and even used as a proxy for identifying plaster production at Neolithic sites (Goren and Goring-Morris, 2008; Malinowski, 2012; Malinsky-Buller et al., 2013). However, to date no study was able to determine their function and whether they were prepared intentionally for the production of calcite-based plasters or were added as part of mixing with the local anthropogenic sediment. Overall, we interpret the plaster found at TRW as a geogenic material made by pulverizing chalk/marl mixed with local archaeological sediment aggregates (some being burnt). Such a mixture of crushed chalk/marl and fire residues was reported in other PPNB sites in the

Southern Levant (Goren and Goldberg, 1991; Goren et al., 2001; Malinowski, 2012). The movement of water through the putty during the preparation and application of the plaster resulted not only in the cementation of the matrix but also in infilling the voids with non-altered clay washed from the local unburnt sediment (figures 9c-d, 10c, 11d and 12c-f).

The use of vegetal temper in plaster production has been reported in the Southern Levant from the Neolithic as well as Bronze and Iron Age tell sites (Goren and Goldberg, 1991; Goren et al., 2001; Shimron, 2004; Friesem and Shahack-Gross, 2013; Goshen et al., 2017; Shahack-Gross, 2018). Previous interpretation of PPNB plaster suggested that vegetal temper was added into a mixture of both lime and un-burnt crushed chalk or marl (Goren and Goldberg, 1991; Goren et al., 2001). Studies of Bronze and Iron Age plasters suggest either adding vegetal temper to lime (Shimron, 2004) or to pulverized rock (Friesem and Shahack-Gross, 2013; Goshen et al., 2017; Shahack-Gross, 2018). The difference of interpretation probably lies in different analytical methods used by the various researchers. Microscopy alone or determination of presence of calcite cannot fully encompass the complexity of plaster production. The use of microscopy together with the FTIR guidelines of Regev et al. (2010a) seems to maximize the interpretational ability. Moreover, presence/absence of microfossils cannot be used to determine application of heat, as demonstrated here experimentally (more below, and see also Daghmehchi et al., 2017).

We suggest that the construction of the P.2000 complex associated with the infant burial in TRW was a relatively rapid and *ad hoc* procedure in which local chalk was first pulverized (resulting in a calcitic powder that formed a matrix along with sub-angular and sub-rounded poorly to moderately sorted rock fragments; see Table 4), then mixed with water and in certain cases also vegetal matter. Soil aggregates (heated and unheated) and bone fragments were either added as temper or were incorporated inadvertently during the preparation procedure. We identified several plastering phases, each with its unique characteristics (Table 4), some separated by soil-based materials. These may either be soil-based mortars or natural accumulation over time between chalk/marl plastering phases. The plaster materials present high variability, pointing out the possibility of different phases of application, each with a different combination of mixing with aggregates (some of them burnt). For example, under the microscope, TRW 16 is very similar to TRW 15 but includes more impurities implying more mixing with aggregates while TRW 17 also presents materials that are relatively similar to TRW 15, but that are clearly separated by a clay-rich infilling of a channel indicating two phases of application. TRW 18 is quite different from the other samples showing higher extent of mixing with local anthropogenic sediment and fire residues with no vegetal tempering. Our reconstruction suggests that the time and labour this procedure of plaster production demanded, could have been

fulfilled by skilful artisans in a relatively short time and minimal effort but nevertheless included several phases of plaster application.

Geoarchaeological implications

The identification and distinction between pyrogenic lime plaster and non-pyrogenic calcite-based plaster made of pulverized rocks mixed (or not) with fire residues is not straightforward. Macroscopically, in the field, they tend to present similar characteristics of cemented light-coloured deposits. Due to the addition of materials such as burnt bones, wood ash, fired-clay fragments and often also burnt chalk, marl or limestone, it is very challenging to visually distinguish between poorly carbonated lime plaster and pulverized-chalk plaster mixed with burnt residues. In such a case, the presence of lime lumps can help to evince the pyrogenic nature of the plaster (Karkanas, 2007; Friesem et al., 2019). Yet, if the lime plaster has been fully recarbonated, the complete transformation into microcrystalline calcite will hamper identification of the pyrogenic nature of plaster when solely relying on petrographic observations (Karkanas, 2007).

The presence of microfossils (e.g., foraminifera and coccoliths) in plasters when using chalk/marl has been already reported from several PPNB (Goren and Goldberg, 1991; Poduska et al., 2012) and historic sites (Goshen et al., 2017; Shahack-Gross, 2018). While in some cases the plasters containing fossils were argued to be pyrogenic lime plaster (Poduska et al., 2012), in other cases the plasters were interpreted as non-fired in the form of pulverized chalk putty (Goshen et al., 2017) or a mixture of burnt and non-burnt materials (Goren and Goldberg, 1991). Our experimentally heated chalk samples provide new indicators to evaluate the exposure of chalk/marl to elevated temperatures based on micromorphological criteria of the appearance of fossils (figure 8). Still, we conclude that among the methods used here, the calcite atomic disorder is the best method to determine whether the plaster is of pyrogenic or geogenic origin (Chu et al., 2008; Regev et al., 2010b, 2010a; Poduska et al., 2012; Goshen et al., 2017; Toffolo et al., 2017; Friesem et al., 2019)(note that stable oxygen and carbon analyses can also make this distinction quite precisely, e.g., van Strydonck et al., 1989).

An important contribution of our study lies in its experimental data that demonstrates that lime plaster paste cannot be produced by heating chalk (local to TRW) to high temperatures. We do not know if this characterises all geological formations composed of chalk. Moreover, we did not find published data regarding the hydraulic properties (or lack of them) of chalk/marl-based plaster. As chalk forms in fertile deep sea it often includes silicates in the form of clay and/or sponge spicules and diatom frustules. It is possible that the use of unheated chalk/marl was preferred in certain instances as the clay within these rocks reduces water permeability, i.e., such plasters had hydraulic properties similar to those of lime plaster. Further studies are required to understand the hydraulic properties of

non-pyrogenic pulverized chalk/marl-based plaster. Overall, our study indicates the variability and complexity within archaeological calcite-based plaster materials. Thus, the archaeological research of plaster materials must go beyond a generic terminology of 'plaster' or 'calcitic mortars' and acknowledge the different production techniques involved in production of plaster materials.

Identification of PPNB mortuary plaster technology

The use of plaster in mortuary contexts in the Southern Levant dates back to the Late Epipalaeolithic Natufian culture. Plaster was found in burials in Eynan ('Ein Mallaha) dating to 15.3-12.9 k cal. BP (Valla et al., 2007) and recently in Nahal Ein Gev II as an extensive cover of a burial ground (c. 16m² and 40 cm thick) dated to 12 k cal. BP (Grosman et al., 2016; Friesem et al., 2019). Given the absence of evidence for plaster in PPNA sites (see Malinsky-Buller et al., 2013 for indirect evidence for lime plaster production based on presence of fired clay aggregates), it is not clear whether PPNB plaster technology is a direct continuum of a Natufian technological tradition or has been reinvented during the PPNB almost two millennia later (Friesem et al., 2019). Nevertheless, the material properties and the production technique of Neolithic mortuary plaster differs from the Natufian one. The PPNB plaster technology exhibits broader utilisation of added materials including the incorporation of heated soil aggregates, wood ash, vegetal temper, bones and dung (e.g., Goren and Goldberg, 1991; Goren et al., 2001; Karkanas, 2007). In terms of mortuary and ritual practices, PPNB plaster has been used not only to cover burials but also for modelling skulls and making figurines and busts (Rollefson, 1990; Goren et al., 2001; Goring-Morris, 2002; Kuijt and Goring-Morris, 2002; Clarke, 2012). Goren et al. (2001) argued that despite some variation in plaster production, the technological skills and knowledge seem to be rather similar across the various uses of plaster during the PPNB and suggested to view it as pyrogenic lime plaster. Goren and Goldberg (1991) reported the presence of pulverized chalk plaster mixed with vegetal temper and some burnt chalk fragments and ash, presenting similarity to the plaster from TRW. They concluded, based on micromorphological observations, that burnt lime was not used in all plaster samples and that when it was in use it did not exceed 30% of the matrix. However, they still defined some of these samples as pyrogenic lime plaster. Clarke (2012) mentioned the use of pyrogenic lime plaster for mortuary practices and suggested that non-pyrogenic calcite-based plaster was used alongside pyrogenic lime plasters for architectural purposes.

To date, most PPNB plaster materials are still interpreted based on field observations or micromorphological analysis. Unfortunately, very few studies applied the FTIR grinding curve method to study PPNB plasters, presenting values that range between geogenic and pyrogenic origins of different plasters. However, these plasters were interpreted as lime plaster showing in some cases values that are associated with more atomically ordered calcite due to mixing with unburnt limestone

or chalk fragments and local sediment (Chu et al., 2008; Regev et al., 2010a; Poduska et al., 2012; Toffolo et al., 2017). We suggest that the majority of the plaster materials of feature P.2000 in TRW are not lime plaster, but rather an impure non-pyrogenic (geogenic) calcite-based plaster. Thus, the case study from TRW provides new data regarding an overlooked aspect of plaster production during the PPNB and demonstrates the necessity for more mineralogical studies via infrared spectroscopy in tandem with micromorphology to be carried out on PPNB plasters in order to determine the production technology and better understand the complexity within Neolithic plaster production.

Social implications of PPNB mortuary plaster production in the Southern Levant

The production of pyrogenic lime plaster during the PPNB has been suggested to evince significant communal effort based on the large amount of estimated fuel needed for such endeavours (Garfinkel, 1987; Rollefson, 1990; Rollefson and Köhler-Rollefson, 1992). However, this view has been challenged, arguing that PPNB plaster production should be seen as a more casual, limited activity in which lime was used very frequently, but in small quantities which did not require intensive labour (Goren and Goldberg, 1991; Goren et al., 2001; Karkanas, 2007; Goren and Goring-Morris, 2008; Rollefson, 2014). Goren and Goldberg (1991) argued that full-time specialists would not necessarily be required for the production of lime plaster. Goren et al. (2001) suggested that lime plaster technology was disseminated in the form of communicated general knowledge, rather than the actual physical movement of artisans from one site to another, but they speculated that skull plastering was practiced only by a limited array of individuals fulfilling such roles within any given community.

Based on the absence of evidence for lime plaster production in some PPNB sites in the Southern Levant, Clarke (2012) argued that access to the pyrotechnological knowledge and skills of lime plaster production was unequal. She supports her argument by stating that lime plaster production was costly in terms of time and fuel and would have required a degree of knowledge transmission. While some cases of lime plaster production provide evidence for the use of kilns in order to burn carbonate rocks over several hours or even days (Goren and Goring-Morris, 2008; Toffolo et al., 2017), the majority of studied PPNB plasters exhibit partially burnt chalk, marl or limestone that could either be obtained by using an open fire for only a few hours, as demonstrated by the experiments of Karkanas (2007), or that they are actually non-fired or only partially burnt plasters mixed with burnt rocks, fired clay and ashes. It is very possible that many of the so-called 'lime' plasters are actually non-pyrogenic/geogenic plasters, only partially burnt and/or mixed with some burnt materials. This calls for a re-consideration of the social, ecological and technological aspects that plaster production played in PPNB societies of the Southern Levant.

It is impossible to reconstruct how and who exactly produced plaster in mortuary PPNB contexts. However, we suggest that the practice of non-pyrogenic plaster production was part of a burial ritual that could have been completed with significantly less effort than producing lime plaster, and potentially carried out by a single person over a relatively short time. Our results do not seem to differ significantly from the data reported by other geoarchaeological studies of PPNB plaster (Goren and Goldberg, 1991; Goren et al., 2001; Chu et al., 2008; Regev et al., 2010a; Poduska et al., 2012; Toffolo et al., 2017). We argue for a more widespread use of non-pyrogenic calcite-based plaster than previously suggested, not only in architectural but also in mortuary contexts. The knowledge and skills to produce non-pyrogenic calcite-based plaster which visibly (i.e., colour) and physically (i.e., hardness, possible water-proofing) resembles pyrogenic lime plaster, but produced with less effort, should be regarded as an important technological innovation. The spread of this innovation must have held important social implications as it allowed the production of the much used plaster during the PPNB in less effort and requiring no fuel resources to produce lime. In addition, following on Clarke's (2012) argument for the enchanting role of plaster during the PPNB due to its visual properties, especially its whiteness and redness, the plasters from TRW, even though not being lime plaster (i.e., non-pyrogenic), seem to follow Clarke's (2012) description by also presenting these different bright white and red colours. Based on our field observations it is unlikely that the p.2000 plaster complex was left visible for a long time following the burial, but it was certainly visible during the burial.

Whether the knowledge and skills for producing non-pyrogenic calcite-based plaster were shared by a limited circle of people that had a particular social status and ritual role in PPNB societies, or were a common practice shared by many allowing more equal access to this technology and ritual, is beyond the scope of this study. Furthermore, it is not clear whether the production of non-pyrogenic chalk/marl based plaster, as opposed to pyrogenic lime plaster, held not only different social meanings but also different functional purposes. Future geoarchaeological identification of the different types of plaster at various sites and contexts will provide additional insights into such technological and cultural questions.

Conclusions

The production of plaster requires advanced technological knowledge and skills in order to transform hard rocks into a plastic paste later to become a hard durable material. We show here that the production itself can be done with far less effort than previously suggested. We provide archaeological and experimental evidence for the production of non-pyrogenic calcite-based plaster that was prepared from pulverized chalk/marl and suggest a methodological protocol for high-resolution mineralogical analysis of archaeological plasters and their formation processes. The combination of

FTIR analysis of bulk samples, micro-FTIR and micromorphological analysis of thin sections, augmented by laboratory experiments, allowed us to reconstruct the production of the studied plasters with high certainty. Based on our analysis we conclude that the various plaster materials in TRW are of geogenic origin, made from non-fired pulverized chalk/marl and mixed with various burnt materials including local sediment, heated soil aggregates, bones, and partially-burnt chalk fragments. The integration of our data with other studies of PPNB lime plaster technology shows that the production at TRW is not exceptional and that it is very possible that non-pyrogenic calcite-based plaster in PPNB mortuary contexts was more widespread than previously thought. Thus, PPNB plaster technology demonstrates the establishment and spread of advanced skills and knowledge of material manipulation. We should bear in mind that producing hard, durable plaster with white and red colors in less effort and resources than those needed to produce lime plaster should be regarded as a technological innovation in itself. The presence of non-pyrogenic calcite-based plaster not only in PPNB sites but also in other periods and geographic areas should be further examined as it holds important social, environmental and technological implications. Finally, we encourage future studies to adopt a more accurate terminology and approach to archaeological calcite-based plasters in order to better characterize and understand its variability and complexity.

Acknowledgements

We would like to thank C. French for the use of the FTIR instrument at the McBurney Laboratory for Geoarchaeology at the University of Cambridge, S. Mentzer and C. Miller for the use of the micro-FTIR at the University of Tübingen and J. J. Gottlieb, conservator at the Recanati Institute for Maritime Studies, University of Haifa, for the production of the archaeological and experimental thin sections. We thank the area supervisors during field work: T. Ghraieb, U. Grinberg, A. Haeim and P. Spivak, and K. Krater and E. Krater Gershtein for their work on the skeleton. We also thank A. Tsatskin, N. Shtober-Zisu and R. Linn for their contribution to the project. Work was carried out under Israel Antiquities Authority license number B-291/2004.

References

- Agha, N., Nadel, D., Bar-Oz, G., 2019. New insights into livestock management and domestication at Tel Ro'im West, a multi-layer Neolithic site in the Upper Jordan Valley, Israel. *Journal of Archaeological Science: Reports*. 27, 101991.
- Artioli, G., Angelini, I., 2010. *Scientific methods and cultural heritage: an introduction to the application of materials science to archaeometry and conservation science*. Oxford University Press, Oxford.

- Ayalon, A., Bar-Matthews, M., Goren, Y., 2004. Authenticity examination of the inscription on the ossuary attributed to James, brother of Jesus. *Journal of Archaeological Science*. 31, 1185–1189.
- Bar-Yosef, O., Goring-Morris, A., 1977. Geometric kebaran a occurrences. In: *Prehistoric Investigations in Gebel Maghara, Northern Sinai*. Qedem, Jerusalem, pp. 331–368.
- Berna, F., Behar, A., Shahack-Gross, R., Berg, J., Boaretto, E., Gilboa, A., Sharon, I., Shalev, S., Shilstein, S., Yahalom-Mack, N., Zorn, J.R., Weiner, S., 2007. Sediments exposed to high temperatures: reconstructing pyrotechnological processes in Late Bronze and Iron Age Strata at Tel Dor (Israel). *Journal of Archaeological Science*. 34, 358–373.
- Bocquentin, F., Khalaily, H., Bar-Yosef Mayer, D.E., Berna, F., Biton, R., Boness, D., Dubreuil, L., Emery-Barbier, A., Greenberg, F., Goren, Y., Horwitz, L.K., Dosseur, G. Le, Lernau, O., Mienis, H.K., Valentin, B., Samuelian, N., 2014. Renewed Excavations at Beisamoun: Investigating the 7th Millennium cal. BC of the Southern Levant. *Journal of the Israel prehistoric Society*. 44, 5–100.
- Boynton, R.S., 1980. *Chemistry and technology of lime and limestone*. Wiley, New-York.
- Chu, V., Regev, L., Weiner, S., Boaretto, E., 2008. Differentiating between anthropogenic calcite in plaster, ash and natural calcite using infrared spectroscopy: implications in archaeology. *Journal of Archaeological Science*. 35, 905–911.
- Clarke, J., 2012. *Decorating the Neolithic: an Evaluation of the Use of Plaster in the Enhancement of Daily Life in the Middle Pre-pottery Neolithic B of the Southern Levant*. Cambridge Archaeological Journal. 22, 177–186.
- Daghmehchi, M., Guido, A., Mastandrea, A., Salahi, M.A., Omrani, M., Nokandeh, J., 2017. Thermal analysis of ancient ceramics using the microchemical and microstructural alterations of foraminifera. *Materials Characterization*. 130, 81–91.
- Eisenberg, E., Gopher, A., Greenberg, R., 2001. *Tel-Teo; A Neolithic, Chalcolithic and Early Bronze Age site in the Hula Valley*. Israel Antiquity Authority, Jerusalem.
- Eshed, V., Nadel, D., 2015. Changes in burial customs from the Pre-Pottery to the Pottery Neolithic periods in the Levant: The case-study of Tel Roim West, Northern Israel. *Paléorient*. 41, 115–131.
- Fazekas, I., Kósa, F., 1978. *Forensic fetal osteology*. Akadémiai Kiadó, Budapest.

- Friesem, D., Shahack-Gross, R., 2013. Area J. Part V: Analyses of sediments from the Level J-4 temple floor. In: Finkelstein, I., Ussishkin, D., Cline, E.H. (Eds.), *Megiddo V: The 2004-2008 Seasons Volume 1*. Tel Aviv University, Tel-Aviv, pp. 143–152.
- Friesem, D.E., Abadi, I., Shaham, D., Grosman, L., 2019. Lime plaster cover of the dead 12,000 years ago – new evidence for the origins of lime plaster technology. *Evolutionary Human Sciences*. 1, e9.
- Garfinkel, Y., 1987. Burnt lime products and social implications in the Pre-Pottery Neolithic B villages in the Near East. *Paléorient*. 13, 69–76.
- Getzov, N., 2008. Ha-Goshrim. In: Stern, E. (Ed.), *The New Encyclopedia of Archaeological Excavations in the Holy Land*. Israel Exploration Society and Simon and Schuster, Jerusalem, pp. 1759–1761.
- Goren, Y., Ayalon, A., Bar-Matthews, M., Schilman, B., 2004. Authenticity Examination of the Jehoash Inscription. *Tel-Aviv*. 31, 3–16.
- Goren, Y., Goldberg, P., 1991. Petrographic Thin Sections and the Development of Neolithic Plaster Production in Northern Israel. *Journal of Field Archaeology*. 18, 131–140.
- Goren, Y., Goring-Morris, A.N., 2008. Early pyrotechnology in the Near East: Experimental lime-plaster production at the Pre-Pottery Neolithic B site of Kfar HaHoresh, Israel. *Geoarchaeology*. 23, 779–798.
- Goren, Y., Goring-Morris, A.N., Segal, I., 2001. The Technology of Skull Modelling in the Pre-Pottery Neolithic B (PPNB): Regional Variability, the Relation of Technology and Iconography and their Archaeological Implications. *Journal of Archaeological Science*. 28, 671–690.
- Goring-Morris, A.N., Goldberg, P., Goren, Y., Baruch, U., Bar-Yosef, D.E., 1997. Saflulim: A Late Natufian Base Camp in the Central Negev Highlands, Israel. *Palestine Exploration Quarterly*. 131, 36–64.
- Goring-Morris, N., 2002. The Quick and the Dead. In: Kuijt, I. (Ed.), *Life in Neolithic Farming Communities*. Springer, Boston, pp. 103–136.
- Goring-Morris, N., Horwitz, L.K., 2007. Funerals and feasts during the Pre-Pottery Neolithic B of the Near East. *Antiquity*. 81, 902–919.
- Goshen, N., Yasur-Landau, A., Cline, E.H., Shahack-Gross, R., 2017. Palatial architecture under the microscope: Production, maintenance, and spatiotemporal changes gleaned from plastered

- surfaces at a Canaanite palace complex, Tel Kabri, Israel. *Journal of Archaeological Science: Reports*. 11, 189–199.
- Gourdin, W.H., Kingery, W.D., 1975. The Beginnings of Pyrotechnology: Neolithic and Egyptian Lime Plaster. *Journal of Field Archaeology*. 2, 133–150.
- Grosman, L., Munro, N.D., Abadi, I., Boaretto, E., Shaham, D., Belfer-Cohen, A., Bar-Yosef, O., 2016. Nahal Ein Gev II, a late natufian community at the sea of galilee. *PLoS ONE*. 11.
- Haaland, M.M., Friesem, D.E., Miller, C.E., Henshilwood, C.S., 2017. Heat-induced alteration of glauconitic minerals in the Middle Stone Age levels of Blombos Cave, South Africa: Implications for evaluating site structure and burning events. *Journal of Archaeological Science*. 86.
- Karkanas, P., 2007. Identification of lime plaster in prehistory using petrographic methods: A review and reconsideration of the data on the basis of experimental and case studies. *Geoarchaeology*. 22, 775–796.
- Khalaily, H., Kuperman, T., Marom, N., Milevski, N., Yegorov, D., 2015. Beisamun: An Early Pottery Neolithic Site in the Hula Basin. *Atiqot*. 82, 1–61.
- Kingery, D.W., Vandiver, P.B., Prickett, M., 1988. The Beginnings of Pyrotechnology, Part II: Production and Use of Lime and Gypsum Plaster in the Pre-Pottery Neolithic Near East. *Journal of Field Archaeology*. 15, 219–243.
- Kuijt, I., Goring-Morris, N., 2002. Foraging, Farming, and Social Complexity in the Pre-Pottery Neolithic of the Southern Levant: A Review and Synthesis. *Journal of World Prehistory*. 16, 361–440.
- Lechevallier, M., 1978. Abou Gosh et Beisamoun, Deux Gisements du VIIe Millénaire avant l'Ère Chrétienne en Israël (Memoires et Travaux du Centre de Recherche Français de Jerusalem 2). : ; . Association Paléorient, Paris.
- Malinowski, R., 2012. Plaster and Lime-Burning Techniques. In: Y. Garfinkel, D. Dag, H. Khalaily, O. Marder, I. Milevski, A.R. (Ed.), *The Pre-Pottery Neolithic B Village of Yiftahel: The 1980s and 1990s Excavations*. ex oriente, Berlin, pp. 229–241.
- Malinsky-Buller, A., Birkenfeld, M., Aladjem, E., Givol-Barzilai, Y., Bonnes, D., Goren, Y., Yeshurun, R., 2013. Another piece in the puzzle - A new PPNA site at Bir el-Maksur (Northern Israel). *Paléorient*. 39, 155–172.
- Maresh, M.M., 1970. Measurements from roentgenograms. In: McCammon, R.W. (Ed.), *Human*

- Growth and Development. C.C. Thomas, Springfield IL, pp. 157–200.
- Nadel, D., Nadler-Uziel, M., 2011. Is the PPNC really different? The flint assemblages from three layers at Tel Roim West, Hula Basin. In: Healey, E., Campbell, S., Maeda, O. (Eds.), *The State of the Stone. Terminologies, Continuities and Contexts in Near Eastern Lithics (Studies in Early Near Eastern Production, Subsistence, and Environment 13)*. ex oriente, Berlin, pp. 243–256.
- Nativ, A., Rosenberg, D., Nadel, D., 2014. The Southern tip of the Northern Levant? The Early Pottery Neolithic assemblage of Tel Ro'im West, Israel. *Paléorient*. 40, 99–115.
- Perrot, J., 1966. Le gisement Natoufien de Mallaha (Eynan), Israel. *L'anthropologie*. 70, 437–484.
- Perrot, J., Ladiray, D., 1988. *Les Hommes de Mallaha (Eynan), Israel, Mémoires e. ed. Association Paléorient, Paris.*
- Poduska, K.M., Regev, L., Berna, F., Mintz, E., Milevski, I., Khalaily, H., Weiner, S., Boaretto, E., 2012. Plaster Characterization At the Ppnb Site of Yiftahel (Israel) Including the Use of 14 C : Implications for Plaster Production , Preservation , and Dating. *Radiocarbon*. 54, 887–896.
- Regev, L., Poduska, K.M., Addadi, L., Weiner, S., Boaretto, E., 2010a. Distinguishing between calcites formed by different mechanisms using infrared spectrometry: Archaeological applications. *Journal of Archaeological Science*. 37, 3022–3029.
- Regev, L., Zukerman, A., Hitchcock, L., Maeir, A.M., Weiner, S., Boaretto, E., 2010b. Iron Age hydraulic plaster from Tell es-Safi/Gath, Israel. *Journal of Archaeological Science*. 37, 3000–3009.
- Rollefson, G.O., 1990. The uses of plaster at Neolithic 'Ain Ghazal, Jordan. *Archaeomaterials*. 4, 33–54.
- Rollefson, G.O., 2014. Recalibrating 'Ain Ghazal. In: Kafafi, Z., Maraqten, M. (Eds.), *A Pioneer of Arabia: Studies in the Archaeology and Epigraphy of the Levant and the Arabian Peninsula*. La Sapienza, Rome, pp. 305–318.
- Rollefson, G.O., Köhler-Rollefson, I., 1992. Early neolithic exploitation patterns in the Levant: Cultural impact on the environment. *Population and Environment*. 13, 243–254.
- Rollefson, G.O., Simmons, A.H., Kafafi, Z., 1992. Neolithic Cultures at 'Ain Ghazal. *Journal of Field Archaeology*. 19, 443–470.
- Rosenberg, D., Assaf, A., Eyal, R., Gopher, A., 2006. Beisamoun: The Wadi Rabah occurrences. *Journal of the Israel Prehistoric Society*. 36, 129–137.

- Schaefer, M., Black, S.M., Scheuer, L., 2009. Juvenile osteology : a laboratory and field manual. Academic.
- Segev, A., Sass, E., 2009. Geological Map of Israel, 1:50 000-Atlit Sheet Israel Geological Survey Map.
- Shahack-Gross, R., 2018. Micromorphological Insights into Construction Materials and their Manufacture Technology at Tell es-Safi/Gath. In: Shai, I., Chadwick, J.R., Hitchcock, L., Dagan, A., McKinny, C., Uziel, J. (Eds.), Tell It in Gath. Studies in the History and Archaeology of Israel. Ägypten und Altes Testament 90, Münster, pp. 799–810.
- Shimron, A.E., 2004. Section I: selected plaster and glassy samples. In: Ussishkin, D. (Ed.), The Renewed Archaeological Excavations at Lachish (1973–1994). Institute of Archaeology, Tel Aviv University, Tel-Aviv, pp. 2620–2653.
- Shoval, S., 2003. Using FT-IR spectroscopy for study of calcareous ancient ceramics. *Optical Materials*. 24, 117–122.
- Sneh, A., Weinberger, R., 2014. Major Structures of Israel and Environs, scale 1: 500,000. Geological Survey of Israel, Jerusalem.
- Stoops, G., 2003. Guidelines for analysis and description of soil and regolith thin sections., Guidelines for analysis and description of soil and regolith thin sections. Soil Science Society of America Inc., Madison, WI.
- Toffolo, M.B., Ullman, M., Caracuta, V., Weiner, S., Boaretto, E., 2017. A 10,400-year-old sunken lime kiln from the Early Pre-Pottery Neolithic B at the Neshar-Ramla quarry (el-Khirbe), Israel. *Journal of Archaeological Science: Reports*. 14, 353–364.
- Valla, F.R., Khalaily, H., Valladas, H., Kaltnecker, E., Bocquentin, F., Cabellos, T., Bar-Yosef Mayer, D.E., Le Dosseur, G., Regev, L., Chu, V., Weiner, S., Boaretto, E., Samuelian, N., Valentin, B., Delerue, S.E., Poupeau, G., Bridault, A., Rabinovich, R., Simmons, T., Zohar, I., Ashkenazi, S., Delgado Huertas, A., Spiro, B., Mienis, H.K., Rosen, A.M., Porat, N., Belfer-Cohen, A., 2007. Les Fouilles de Ain Mallaha (Eynan) de 2003 à 2005: Quatrième Rapport Préliminaire. *Journal of the Israel prehistoric Society*. 37, 135–379.
- van Strydonck, M.J.Y., Dupas, M., Keppens, E., 1989. Isotopic Fractionation of Oxygen and Carbon in Lime Mortar Under Natural Environmental Conditions. *Radiocarbon*. 31, 610–618.
- Villagran, X.S., Strauss, A., Miller, C., Ligouis, B., Oliveira, R., 2017. Buried in ashes: Site formation processes at Lapa do Santo rockshelter, east-central Brazil. *Journal of Archaeological Science*. 77, 10–34.

Weiner, S., 2010. *Microarchaeology: Beyond the Visible Archaeological Record*. Cambridge University Press, Cambridge.

Table1

Table 1 –Bulk mineralogical composition of archaeological sediment samples determined by FTIR. Values of the calcite v2 and v4 are presented in normalised absorbance units [n.a.u; based on the method of Regev et al. 2010] displaying the range obtained through gradual grinding for samples with sufficient amount of calcite.

Legend for minerals: Cl=clay; Ca=calcite.

Sample	Description	Major minerals	v2	v4
TRW-1	Orange material from the top of the block	Cl>>Ca	-	-
TRW-2	Brown material between the orange deposit at the top of block	Cl>Ca	373-299	135-98
TRW-3	White yellowish material	Ca>>>Cl	457-361	158-99
TRW-4	Grey material	Ca>>>Cl	444-287	173-71
TRW-5	Soft yellow material with blocky shape soft material	Ca>>>Cl	453-338	220-107
TRW-6	Brown sediment below the soft yellow block	Cl>>Ca	-	-
TRW-7	White pink material	Ca>>Cl	485-335	229-111
TRW-8	White material	Ca>>Cl	445-299	165-80
TRW-9	Brown-orange and pink material	Cl>Ca	403-327	157-102
TRW-10	Mixed white material	Cl, Ca	414-311	164-89
TRW-11	White granular material	Ca	496-290	244-80
TRW-12	Massive blocky brown material	Cl>>>Ca	-	-
TRW-13	Grey material	Ca	577-335	207-80
TRW-14	Orange material below grey	Cl, Ca	331-280	98-75

Table 2 – Micromorphological description and interpretation of archaeological deposits in thin sections.

Sample	Key micromorphological observations	Interpretation
TRW-15	Moderately sorted dense calcite-rich groundmass showing some areas with embedded fossils and pelletal structure. Complex microstructure with chambers, vesicles and vughs, but mainly channels and fissures infilled with clay hypocoating, and moldic voids after vegetal temper. The matrix is mixed with rubified clay (ceramic-like) aggregate and bones.	Plaster mad of pulverized-chalk mixed with vegetal temper, clay, bone and ceramic-like fragments
TRW-16	Similar to TRW-15. In addition, showing large sediment clasts composed of clay-rich groundmass with fine silt sub-angular quartz and organic matter. Clay is being washed away from the clasts forming hypocoating of voids in the calcite-rich matrix.	Similar to TRW-15 but more mixed with the local sediment but without vegetal temper
TRW-17	Sharp contact between (1) yellowish calcite-rich dense matrix and (2) a similar matrix but more clay-rich and with iron staining and extensive clay infilling and hypocoating of voids (mainly channels). The contact itself is composed of a channel infilled with clay.	Two phases of plaster application. Some parts of the plaster might represent burnt pulverized chalk mixed with unburnt chalk fragments
TRW-18	Diffused contact between (1) poorly sorted calcite-rich matrix with high abundance of clay-rich clasts, burnt and half-burnt chalk fragments (some with a phosphatised rim), bones and wood ash pseudomorphs, and (2) a clay-rich groundmass with fine silt sub-angular quartz and organic matter mixed with micritic calcite displaying complex microstructure with chambers, channels, vesicles and vughs, clay infilling and hypocoating of voids.	Plaster mixed with partly burnt residues above the local unburnt sediment

Table 3 – Assessment of presence/absence of heat altered clay minerals using micro-FTIR. Note that heat alteration of clay minerals can be identified using this method (based on Berna et al. 2007) if they have been exposed to temperatures above 500°C. Presence of one absorbance band indicates heat alteration while more bands indicate slightly- and non-altered clay minerals in the studied samples.

Sample	Description	Absorption bands indicative of altered/non-altered clay minerals (cm ⁻¹)	Interpretation
TRW 15-1	Clay aggregate	3620	Altered
TRW 15-2	Clay infilling	3622, 3695	Non-altered
TRW 16-1	Clay aggregate	3622, 3695	Non-altered
TRW 16-2	Small clay aggregate	3620, 3695	Non-altered
TRW 17-1	Clay aggregate	3620	Altered
TRW 17-2	Clay infilling	3622, 3695	Non-altered
TRW 17-3	Small clay aggregate	3620, small shoulder at 3695	Slightly altered
TRW 17-4	Clay-rich matrix	3620, 3695	Non-altered
TRW 18-1	Clay aggregate	3620, small shoulder at 3695	Slightly altered
TRW 18-2	Clay matrix	3625, 3695	Non-altered
TRW 18-3	Clay aggregate	3620, 3692	Non-altered
TRW 18-4	Small clay aggregate	3620, small shoulder at 3690	Slightly altered
TRW 18-5	Small clay aggregate	3620	Altered

Table 4– Summary of the variability in plaster materials based on micromorphological properties.

	15 (white)	16 (grey)	17a (grey)	17b (red)	18a (grey)	18b (red)
Impurities	+	++	+	+	+	-
Vegetal temper	+	-	+	++	-	-
Sorting of rock fragments	Poor	Poor	Moderate	Poor	Moderate	Good
Roundedness of rock fragments	Sub-angular to sub-rounded	Sub-angular to sub-rounded	Mostly sub-rounded	Sub-angular to sub-rounded	Sub-angular to sub-rounded	Sub-angular

1 **Figure captions:**

2

3 **Figure 1:** (a) Location map, with inset showing major Neolithic sites in the Hula Valley;
4 (b) The excavation areas at the site, with the red star marking the location of burial 2116.

5

6 **Figure 2:** The unique feature above the complex associated with the burial (B2116+P2000), the red
7 arrow marks the location of the baby burial (under feature 2107). Only one such stone feature was
8 found in the entire site

9

10 **Figure 3:** Schematic drawings of the burial (B2116) and the associated plaster complex (P2000). (a) A
11 view from the top; (b) a profile view. The dashed rectangle in the section marks the block retrieved
12 in the field and studied in the lab.

13

14 **Figure 4:** Four photos of various stages of the excavation of the skeleton

15

16 **Figure 5:** The block during sampling at the University of Haifa. (a) Top view showing the location of
17 bulk samples (TRW-1 to 14). Scale bar is 10 cm; (b) A view of the block's cross section. Scale bar is 10
18 cm; (c) Location of block samples: TRW 15 showing white yellow blocky material (associated with
19 TRW-5), and TRW-16 composed of a grey layer (associated with TRW-4). Scale bar is 20 cm; (d)
20 Location of block samples: TRW 17 showing white pinkish material (associated with TRW-3), and
21 TRW-18 composed of the contact between a grey layer (associated with TRW-13) and brown orange
22 sediment (associated with TRW-14). Scale bar is 20 cm.

23

24 **Figure 6:** Infrared spectra of (a) Taqiye unburned and (b) Taqiye heated to 900°C.

25

26 **Figure 7:** Grinding curves of calcite obtained through FTIR analysis as a proxy for the atomic
27 order/disorder of calcite. The chart displays the end values of the ν_2 and ν_4 infrared absorbance
28 band heights [using normalized absorbance units (n.a.u.)(Regev et al., 2010a)]. Each archaeological
29 sample is coloured according to field observations. The coloured lines are references for
30 experimental plaster, wood ash, chalk and limestone published by Regev et al., 2010a.

31

32 **Figure 8:** Microphotograph of experimental heating of a chalky facies of the Ghareb and Taqiye
33 Formation. In all samples the left photograph is in PPL and the right in XPL. (a-b) Unburned; (c-d)
34 Heated to 400°C. Note the transparent fossil shells in the unburnt and at 400°C; (e-f) Heated to
35 500°C; (g-h) Heated to 600°C. Note the pelletal/crumblly microstructure at 500°C and the vesicles
36 (large round features in the upper and lower right) at 600°C, the yellowish tint of the groundmass
37 and the reddening of the fossil shells (center in h); (i-j) Heated to 800°C; (k-l) Heated to 900°C. Note
38 the bright orange-red fossil shells in PPL and the opaque (isotropic) groundmass in XPL.

39

40 **Figure 9:** TRW-15 microscopic observations. (a) Scan of thin section in PPL; (b) Scan of thin section in
41 XPL. Numbers marks the location of samples analysed by micro-FTIR (Table 3). Number 1 marks non-
42 altered clay infilling of a channel. Number 2 marks a rubified (ceramic-like) altered clay aggregate.
43 The blue circle marks a bone fragment embedded in cemented matrix. Red arrow marks moldic
44 voids after vegetal temper [f]; (c) Microphotogrpah of foraminifera fossils embedded in calcite-rich
45 matrix and channels with clay hypocoating. Photograph is in PPL; (d) Microphotogrpah showing
46 matrix with cemented calcitic-clay groundmass with chalk fragments in pelletal structure and clay
47 hypocoating of voids. Photograph is in PPL; (e) Microphotograph showing a bone (arrow) embedded
48 in calcite rich matrix with vesicles and areas with pelletal structure (top) and clay hypocoating.
49 Photograph is in PPL; (f) Microphotgarph of moldic voids after degradation of vegetal matter used as
50 temper. Photograph is in PPL.

51

52 **Figure 10:** TRW-16 microscopic observations. (a) Scan of thin section in PPL; (b) Scan of thin section
53 in XPL. Numbers marks the location of samples analysed by micro-FTIR (Table 3). Number 1 marks
54 clast of non-altered clay-rich sediment [c]. Number 2 marks a non-altered clay aggregate [d]; (c)
55 Microphotograph showing a large clast of clay-rich sediment with silty quartz with clay being washed
56 away and infilling the channels in the calcite-rich matrix. Photograph is in XPL; (d) Microphotograph
57 of non-altered clay aggregate embedded in calcite-rich matrix showing also various fossils.
58 Photograph is in XPL; (e) Microphotograph of different types of fossils embedded in calcite-rich
59 matrix. Photograph is in PPL; (f) Microphotograph of calcite-rich matrix showing pelletal structure
60 and fossils. Photograph is in PPL.

61

62 **Figure 11:** TRW-17 microscopic observations. (a) Scan of thin section in PPL; (b) Scan of thin section
63 in XPL. The grey matrix is placed on top of the red matrix. Numbers marks the location of samples
64 analysed by micro-FTIR (Table 3). Number 2 marks the sharp contact between calcite-rich matrix
65 (upper right [c]) and similar matrix but richer in clay (lower left [d]). The contact is composed of non-
66 altered clay infilling of a elongated channel [e]. Numbers 1 and 3 mark altered clay aggregates. Red
67 arrow marks moldic voids after vegetal temper [f]; (c) Microphotograph of the calcite-rich matrix
68 showing pelletal structure with a sharp contact made of an elongated channel infilled with clay.
69 Photograph is in PPL; (d) Microphotograph of the matrix displaying clay staining of the groundmass
70 and a fossil. Photograph is in PPL; (e) Microphotograph of the contact between the two matrices
71 composed of an elongated channel infilled with non-altered clay separating a calcite-rich matrix
72 showing a pelletal structure (right) and dense matrix with clay staining and hypocoatings, chalk
73 fragments and moldic voids after vegetal temper (arrow). The contact itself is interpreted as a clay
74 infilling of a channel. Photograph is in XPL; (f) Microphotograph showing moldic voids after vegetal
75 temper and chambers, vesicles and channel voids. Photograph is in PPL.

76

77 **Figure 12:** TRW-18 microscopic observations. (a) Scan of thin section in PPL; (b) Scan of thin section
78 in XPL. The grey matrix is placed on top of the red matrix. Numbers marks the location of samples
79 analysed by micro-FTIR (Table 3). The red circle marks the location of burnt rock fragment and clay
80 aggregate embedded in calcite-rich matrix [c]; (c) Microphotograph of the calcite-rich matrix
81 showing a black burnt chalk fragment and brown clay aggregates. Photograph is in PPL; (d)
82 Microphotograph of clay-rich groundmass with fine silt sub-angular quartz displaying clay
83 hypocoating of channels. Photograph is in XPL; (e) Microphotograph of burnt chalk fragment
84 embedded in calcite-rich matrix with brown clay aggregates. Photograph is in PPL; (f) Close up of the
85 cemented matrix. Photograph is in XPL.

86

87

88

89

Figure 1
[Click here to do a high resolution image](#)

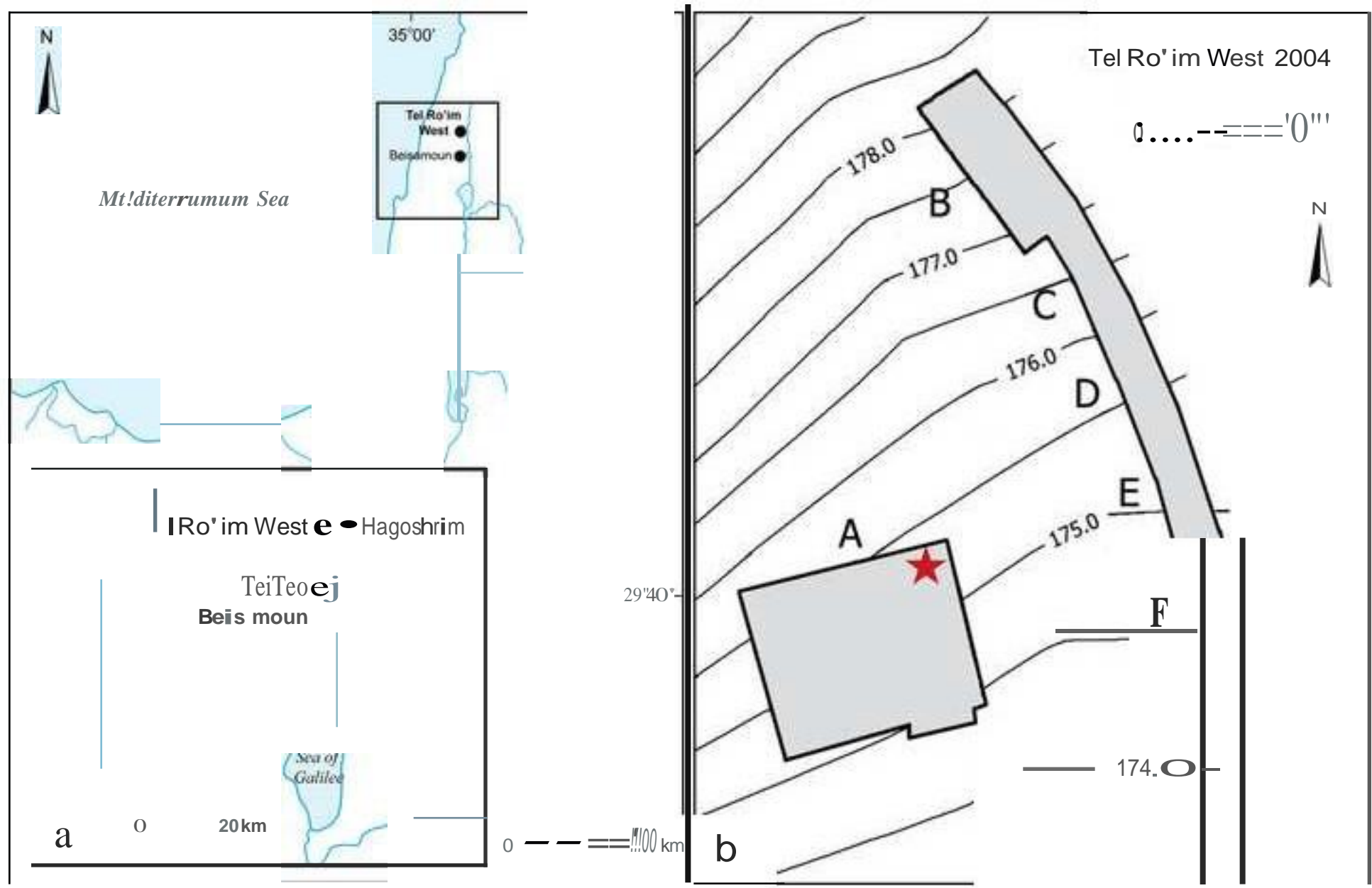


Figure2
[Click here to do high resolution image](#)

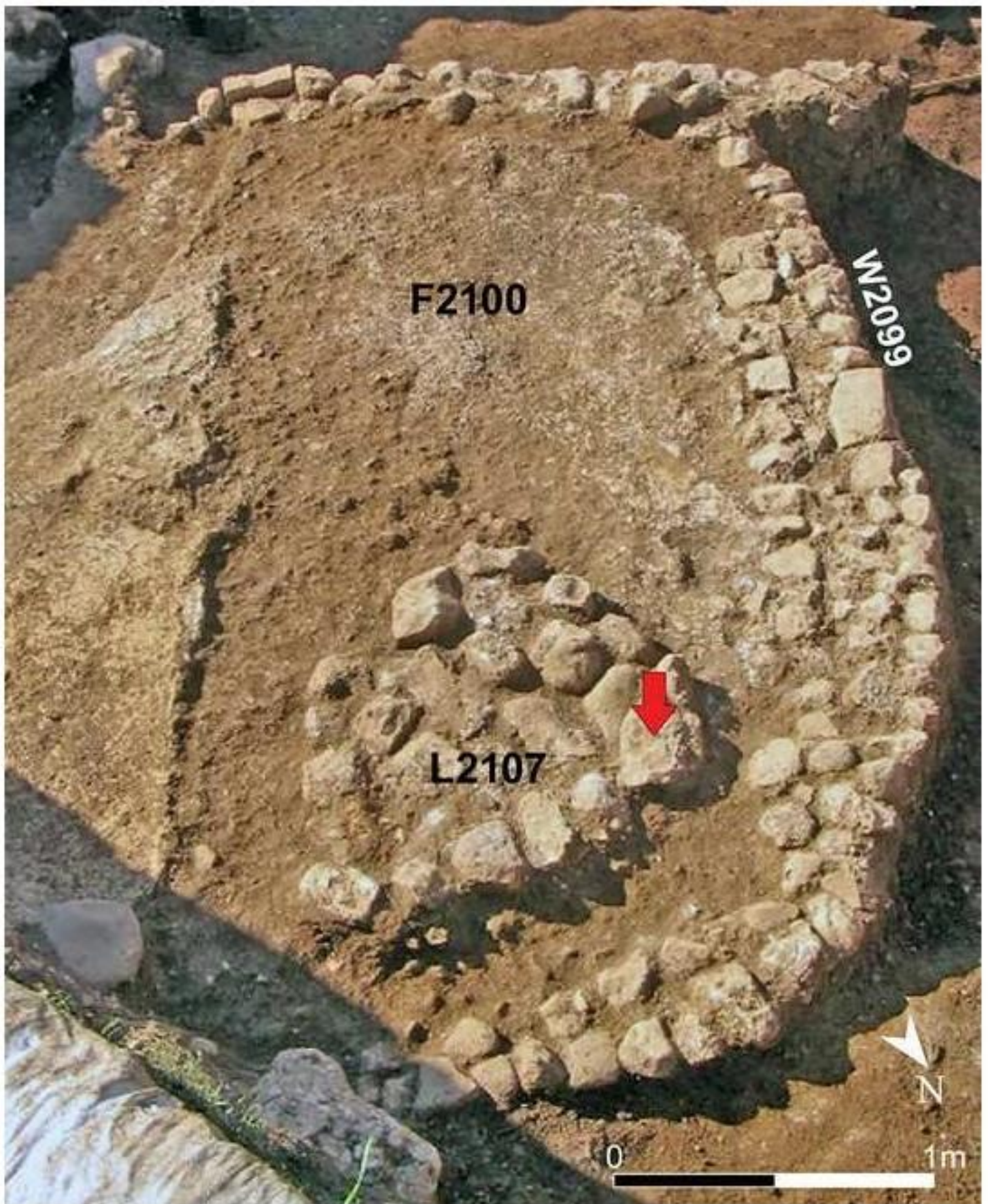


Figure3
[Click here to do high resolution image](#)

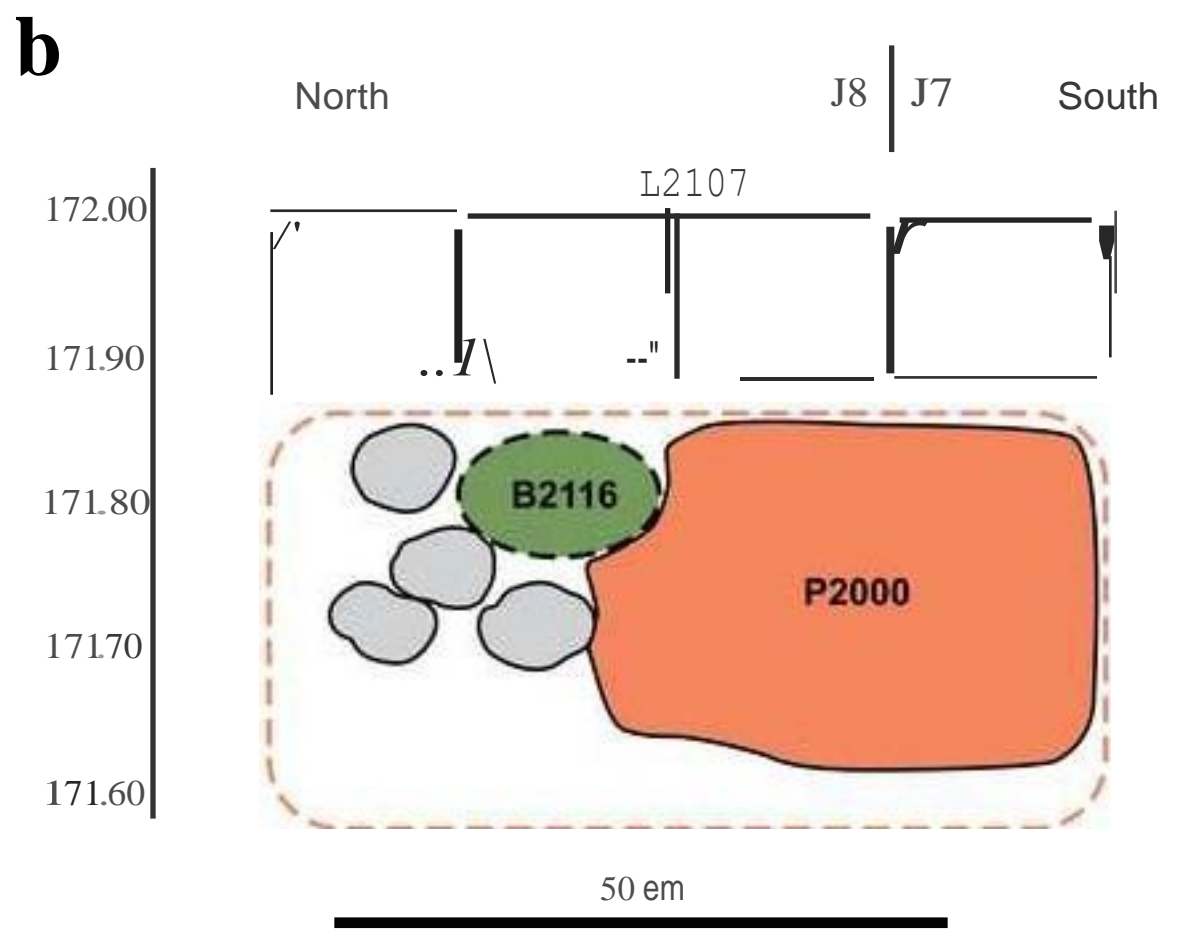
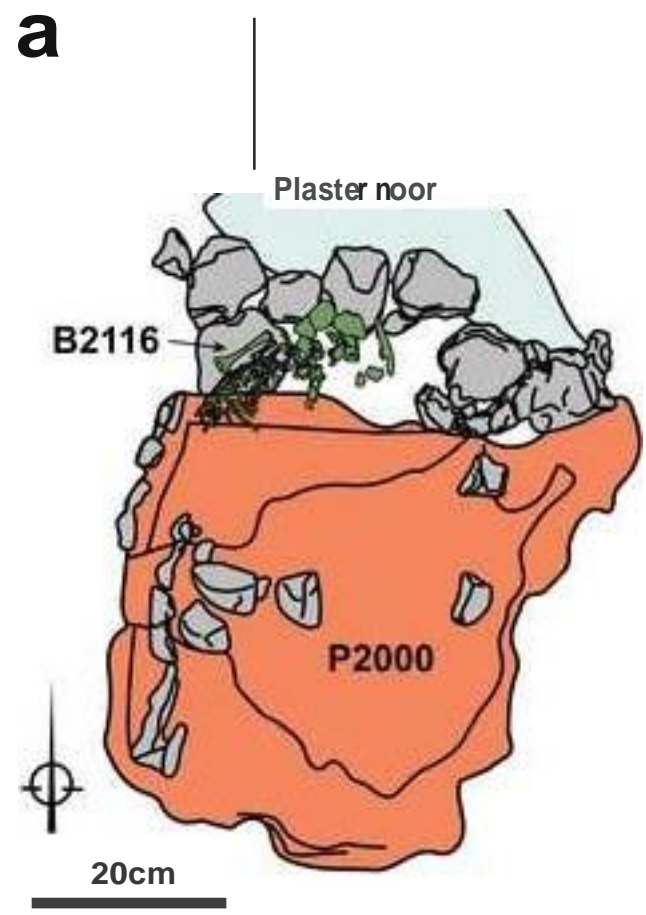
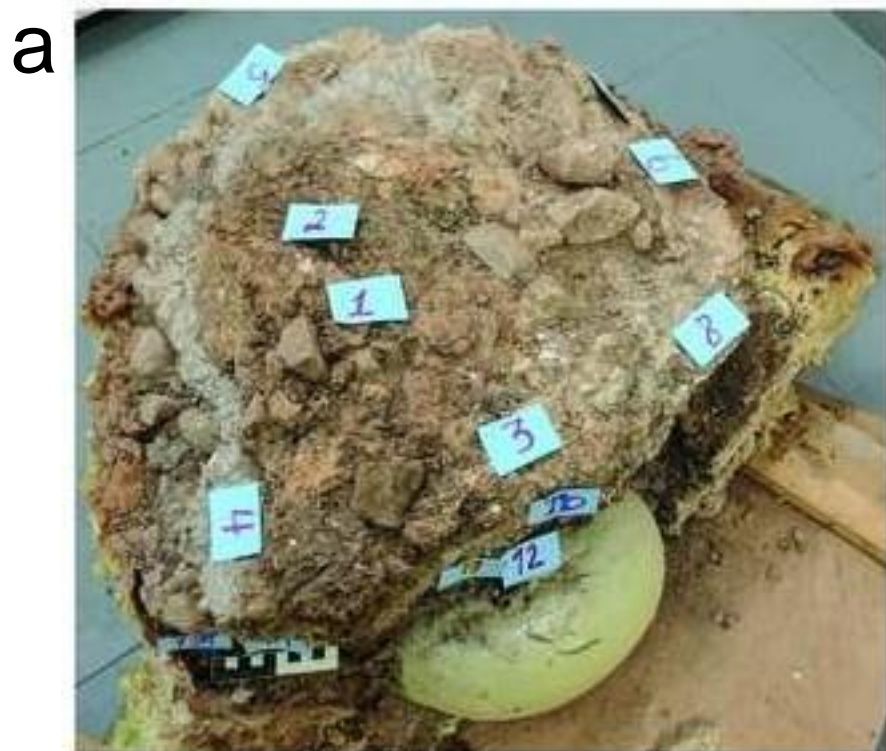
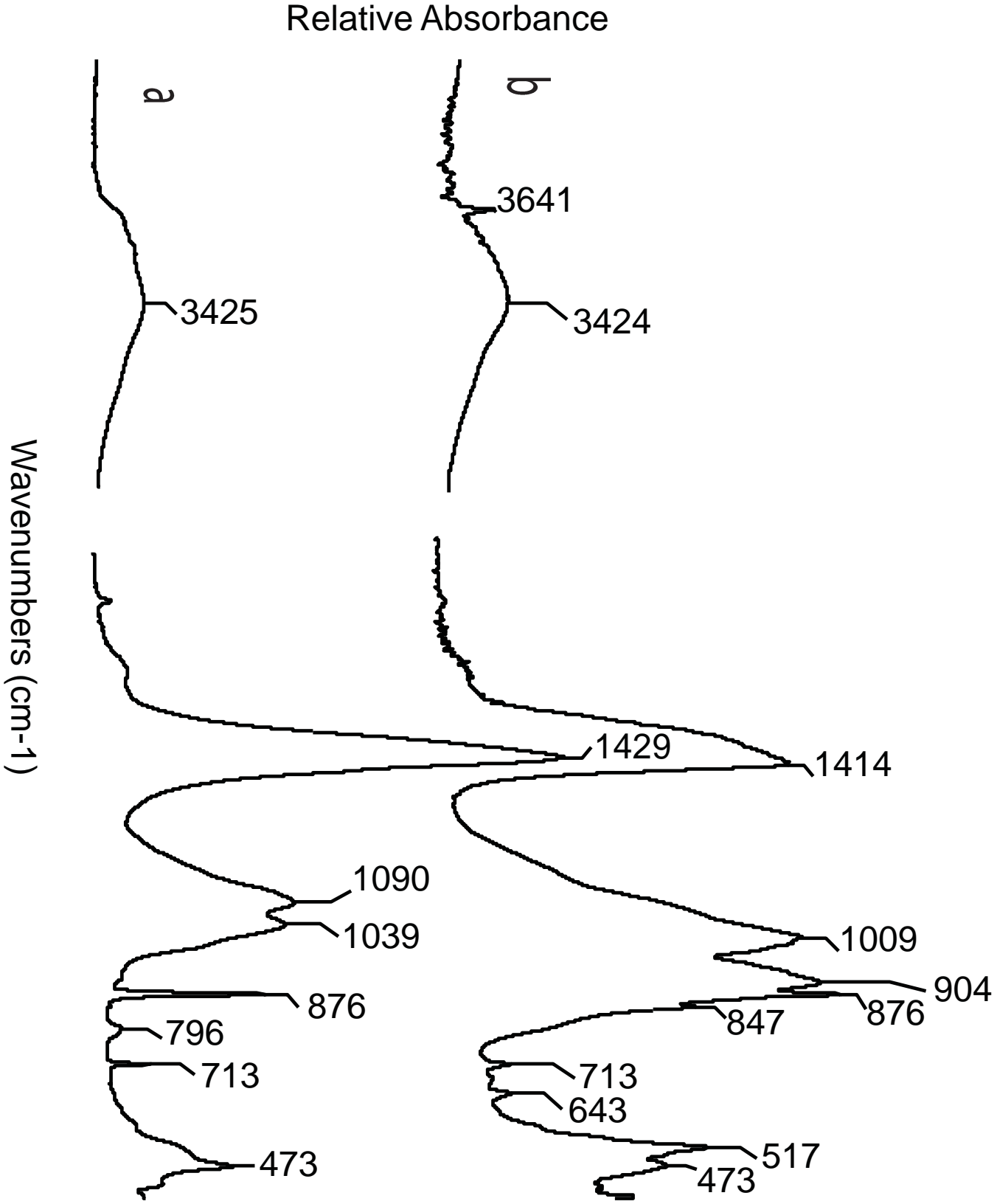


Figure 4
[Click here to do ""loajhigh resolution image](#)

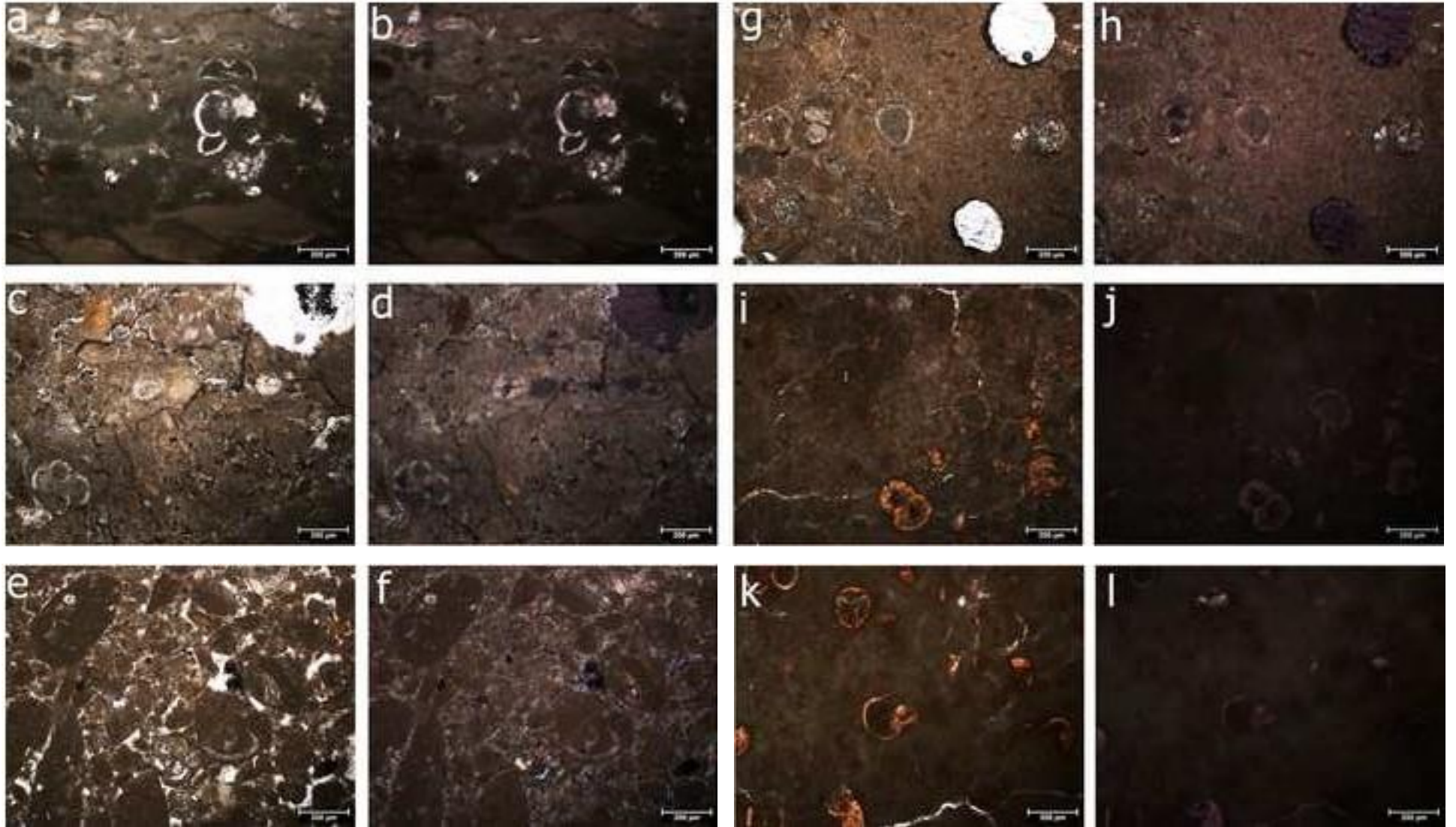


Figure 5
[Click here to do a high resolution image](#)





FigureS
[Click here to do ""loajhigh resolution image](#)



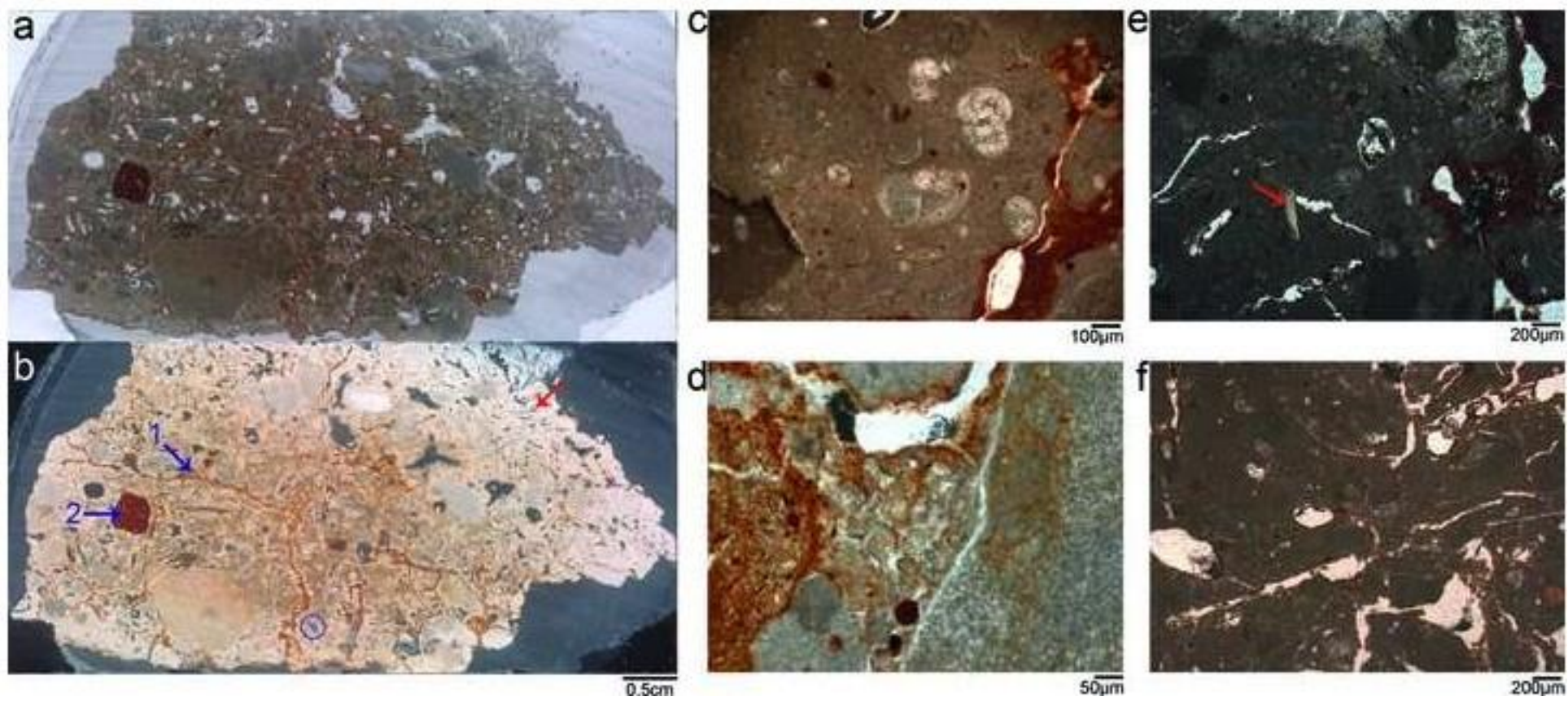


Figure 10
[Click here to do a high resolution image](#)

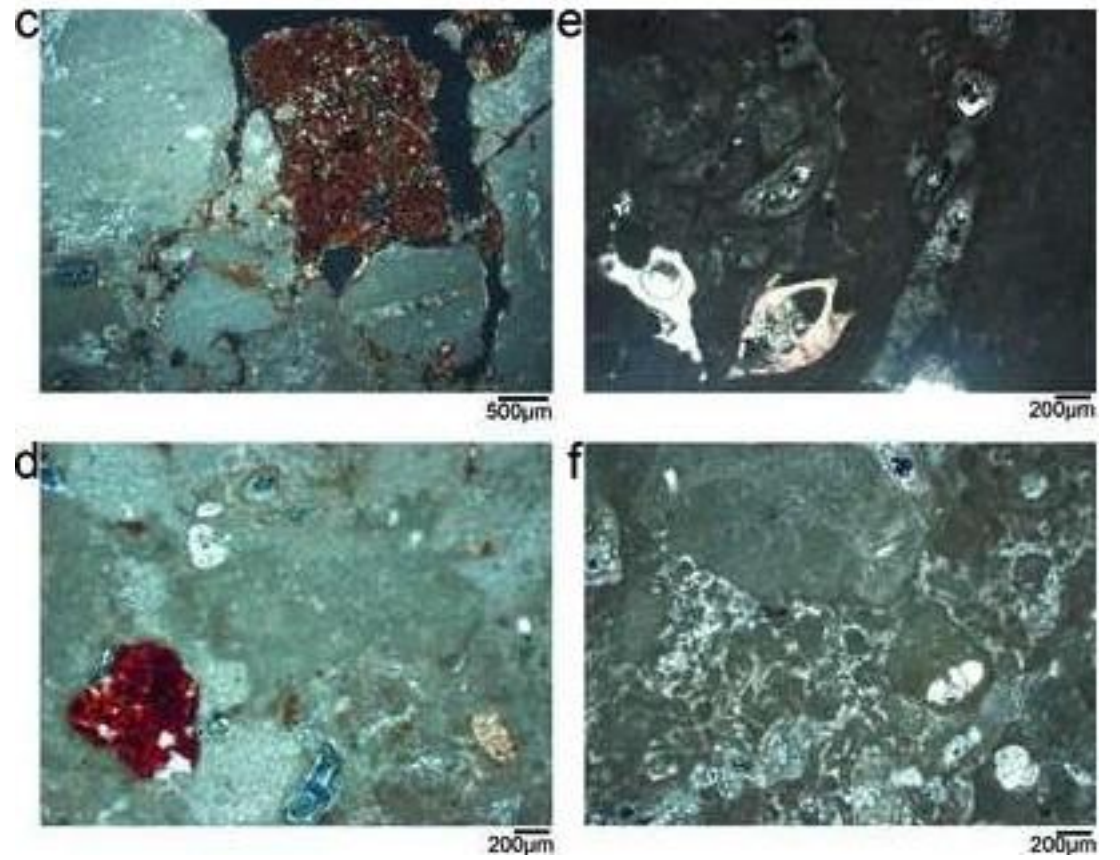
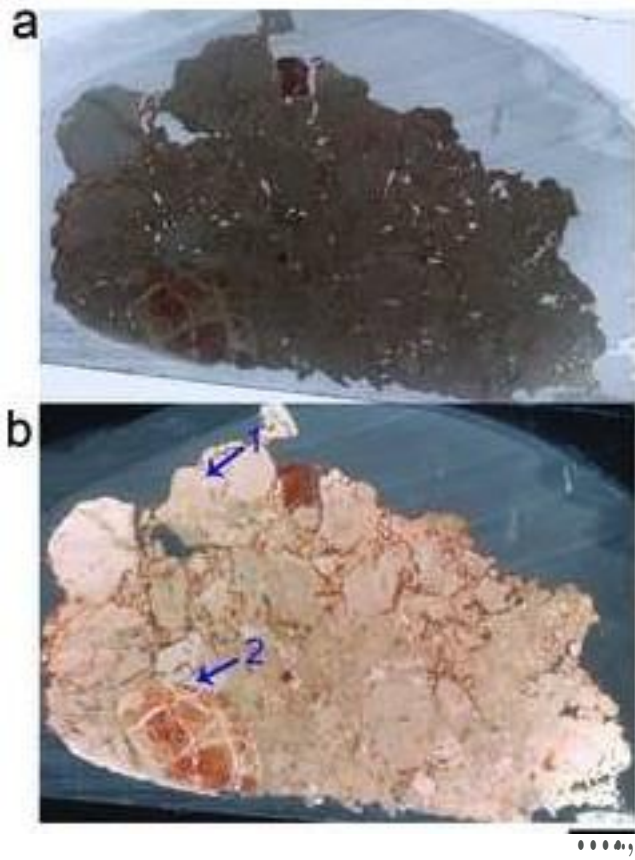


Figure 11
[Click here to do a high resolution image](#)

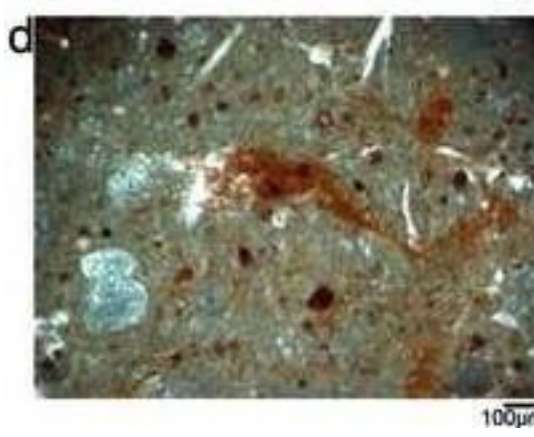
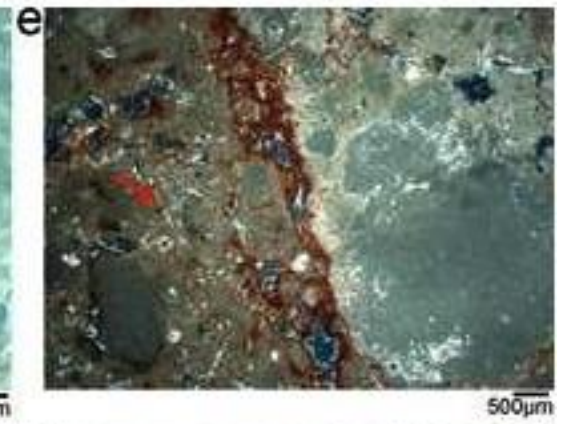
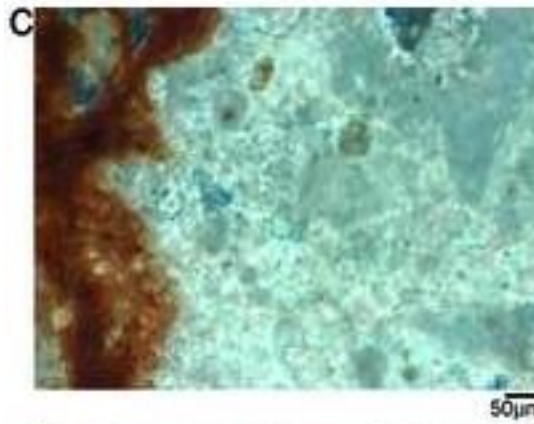
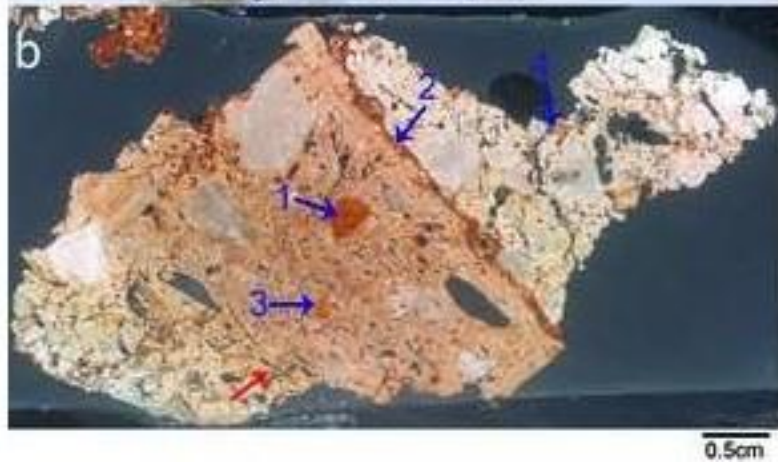
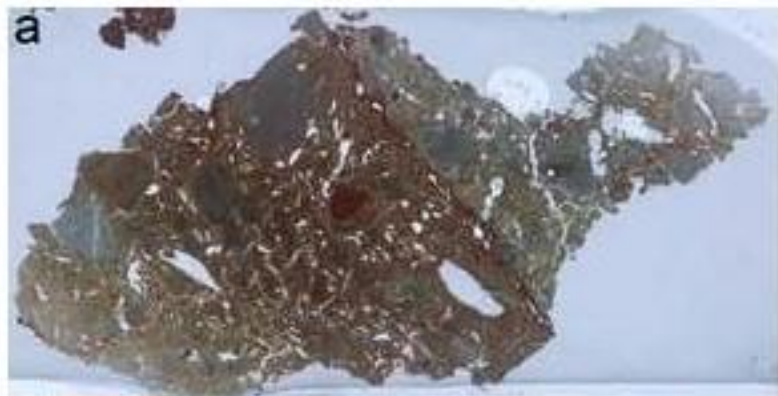


Figure 12
[Click here to do a high resolution image](#)

